Rare copy number variants in *NRXN1* and *CNTN6* increase risk for Tourette syndrome

Alden Y. Huang[1-3], Dongmei Yu[4,5], Lea K. Davis[6,7], Jae-Hoon Sul[1,2], Fotis Tsetsos[8], Vasily Ramensky[1,2], Ivette Zelaya[1-3], Eliana Marisa Ramos[1,2], Lisa Osiecki[4], Jason A. Chen[1-3], Lauren M. McGrath[9], Cornelia Illmann[4], Paul Sandor[10], Cathy L. Barr[11], Marco Grados[12], Harvey S. Singer[12], Markus M. Noethen[13,14], Johannes Hebebrand[15], Robert A. King[16], Yves Dion[17], Guy Rouleau[18], Cathy L. Budman[19], Christel Depienne[20,21], Yulia Worbe[21], Andreas Hartmann[21], Kirsten R. Muller-Vahl[22], Manfred Stuhrmann[23], Harald Aschauer[24,25], Mara Stamenkovic[24], Monika Schloegelhofer[25], Anastasios Konstantinidis[24,26], Gholson J. Lyon[27], William M. McMahon[28], Csaba Barta[29], Zsanett Tarnok[30], Peter Nagy[30], James R. Batterson[31], Renata Rizzo[32], Danielle C. Cath[33], Tomasz Wolanczyk[34], Cheston Berlin[35], Irene A. Malaty[36], Michael S. Okun[36], Douglas W. Woods[37,38], Elliott Rees[39], Carlos N. Pato[40], Michele T. Pato[40], James A Knowles[41], Danielle Posthuma[42], David L. Pauls[4], Nancy J. Cox[6,7], Benjamin M. Neale[4,5,43], Nelson B. Freimer[1,2], Peristera Paschou[8,47], Carol A. Mathews[44,47], Jeremiah M. Scharf[4,5,45,46,47], & Giovanni Coppola[1,2,47], on behalf of the Tourette Syndrome Association International Consortium for Genomics (TSAICG) and the Gilles de la Tourette Syndrome GWAS Replication Initiative (GGRI)

Correspondence should be addressed to J.M.S. (jscharf@partners.org) or G.C. (gcoppola@ucla.edu).

[1]Semel Institute for Neuroscience and Human Behavior, David Geffen School of Medicine, University of California Los Angeles, Los Angeles, California, USA

[2]Department of Psychiatry and Biobehavioral Sciences, University of California, Los Angeles, California, USA

[3]Bioinformatics Interdepartmental Program, University of California, Los Angeles, Los Angeles, California, USA

[4]Psychiatric and Neurodevelopmental Genetics Unit, Center for Human Genetics Research, Department of Psychiatry, Massachusetts General Hospital, Boston, MA, USA

[5]Stanley Center for Psychiatric Research, Broad Institute of MIT and Harvard, Cambridge, MA, USA

[6]Division of Genetic Medicine, Vanderbilt University Medical Center, Nashville, Tennessee, USA

[7]Vanderbilt Genetics Institute, Vanderbilt University Medical Center, Nashville, Tennessee, USA

[8]Department of Molecular Biology and Genetics, Democritus University of Thrace, Greece

[9]Department of Psychology, University of Denver, Denver, Colorado, USA

[10]Toronto Western Hospital, University Health Network and Youthdale Treatment Centres, Department of Psychiatry, University of Toronto, Toronto, Ontario, Canada

[11]Krembil Research Institute, Toronto Western Hospital, University Health Network, Department of Psychiatry, University of Toronto, Toronto, Canada

[12]Johns Hopkins University School of Medicine, Baltimore, Maryland, USA

[13]Department of Genomics, Life & Brain Center, University of Bonn, Bonn, Germany

[14]Institute of Human Genetics, University of Bonn, Bonn, Germany

[15]Department of Child and Adolescent Psychiatry, Psychosomatics and Psychotherapy, University Hospital Essen, University of Duisburg-Essen

[16]Yale Child Study Center, Yale University School of Medicine, New Haven, Connecticut, USA

[17]University of Montréal, Montreal, Canada

[18]Montreal Neurological Institute, Department of Neurology and Neurosurgery, McGill University, Montreal, Quebec, Canada

[19]Hofstra Northwell School of Medicine, Hempstead, New York, USA

[20]Département de Médicine translationnelle et Neurogénétique, IGBMC, CNRS UMR 7104/INSERM U964/Université de Strasbourg, 67400 Illkirch, France

[21]Brain and Spine Institute, UPMC/INSERM UMR_S1127, Paris, France

[22]Clinic of Psychiatry, Social Psychiatry and Psychotherapy, Hannover Medical School, Germany

[23]Institute of Human Genetics, Medical School, Hannover, Germany

[24]Medical University Vienna, Department of Psychiatry and Psychotherapy, Vienna, Austria

[25]Biopsychosocial Corporation, Vienna, Austria

[26]Center for Mental Health Muldenstrasse, BBRZMed, Linz, Austria

[27]Stanley Institute for Cognitive Genomics, Cold Spring Harbor Laboratory, Cold Spring Harbor, New York, USA

[28]Department of Psychiatry, University of Utah, Utah, USA

[29]Institute of Medical Chemistry, Molecular Biology and Pathobiochemistry, Semmelweis University, Budapest, Hungary

[30]Vadaskert Child and Adolescent Psychiatric Hospital, Budapest, Hungary

[31]Children's Mercy Kansas City, Kansas City, Kansas, USA

[32]Dipartimento di Medicina Clinica e Sperimentale, Università di Catania, Catania, Italy

[33]Utrecht University, Department of Clinical Psychology and Altrecht Academic Anxiety Center, Utrecht, the Netherlands

[34]Department of Child Psychiatry, Medical University of Warsaw, Poland

[35]Penn State University College of Medicine, Hershey, Pennsylvania, USA

[36]Department of Neurology and Center for Movement Disorders and Neurorestoration, University of Florida, Gainesville, Florida, USA

[37]Marquette University, Milwaukee, Wisconsin, USA

[38]University of Wisconsin-Milwaukee, Milwaukee, Wisconsin, USA

[39]Medical Research Council Centre for Neuropsychiatric Genetics and Genomics, Cardiff University, Cardiff, Wales, United Kingdom

[40]SUNY Downstate Medical Center, Brooklyn, New York, USA

[41]Department of Psychiatry & Behavioral Sciences, Keck School of Medicine, University of Southern California, Los Angeles, California, USA

[42]Department of Complex Trait Genetics, Center for Neurogenomics and Cognitive Research, VU University Amsterdam, Amsterdam, the Netherlands

[43]Analytic and Translational Genetics Unit, Department of Medicine, Massachusetts General Hospital, Boston, MA, USA

[44]Department of Psychiatry, Genetics Institute, University of Florida, Gainesville, Florida, USA

[45]Department of Neurology, Brigham and Women's Hospital, Boston, MA, USA

[46]Department of Neurology, Massachusetts General Hospital, Boston, MA, USA

[47]These authors jointly directed this work.

Tourette syndrome (TS) is highly heritable, although identification of its underlying genetic cause(s) has remained elusive. We examined a European ancestry sample composed of 2,435 TS cases and 4,100 controls for copy-number variants (CNVs) using SNP microarrays and identified two genome-wide significant loci that confer a substantial increase in risk for TS (*NRXN1*, OR=20.3, 95%CI [2.6-156.2], p=6.0 × 10^{-6}; *CNTN6*, OR=10.1, 95% CI [2.3-45.4], p=3.7 × 10^{-5}). Approximately 1% of TS cases carried one of these CNVs, indicating that rare structural variation contributes significantly to the genetic architecture of TS.

Tourette syndrome (TS) is a complex developmental neuropsychiatric disorder of childhood onset characterized by multiple motor and vocal tics, with an estimated population prevalence of 0.3-0.9%[1]. Twin and family-based studies of TS have repeatedly demonstrated that it is highly heritable (e.g., h^2 of 0.77 in a recent analysis of the Swedish National Patient Register[2]), while analysis of genome-wide SNP data suggests that TS risk is highly polygenic and distributed across both common and rare variation[3]. To date, the TS samples with available genome-wide genotyping have been inadequately sized for common variant association studies of a complex trait. To further characterize the genetic influences on TS, we assessed the impact of rare CNVs on disease risk, as it has been shown repeatedly that such variants contribute to susceptibility for other heritable neurodevelopmental disorders, including intellectual disability (ID), autism spectrum disorder (ASD) and schizophrenia (SCZ)[4].

We genotyped TS cases and ancestry-matched controls on the same genome-wide SNP array platform (Illumina OmniExpress, Supplementary Table 1a). Following standard quality control (QC) steps (Supplementary Table 1b, Supplementary Figure 1, and Supplementary Text), including genotype-based determination of ancestry (Supplementary Figure 2), we analyzed CNVs in a SNP dataset of 6,535 unrelated European ancestry samples, including 2,435 individuals diagnosed with TS (by DSM-IV-TR criteria) and 4,100 healthy controls. To improve specificity, we generated CNV calls with two widely-used Hidden Markov Model (HMM)-based segmentation algorithms, PennCNV[5] and QuantiSNP[6] and retained the intersection of CNVs detected by both methods. We also conducted an additional QC step to test for any differential sensitivity in CNV detection between cases and controls, both within and across batches and sites, by analyzing CNV calls from 11 common HapMap3 CNVs using a sensitive locus-specific intensity clustering method, generating a total of 4,758 non-reference CNV calls across all samples (Supplementary Figure 3). Comparison of these genotypes with our consensus HMM-based calls confirmed the absence of any differential bias in the sensitivity of CNV detection between phenotypic groups whether assessed across all loci (p=0.53, Fisher's exact test) or between individuals (p=0.15, Welch's *t*-test, Supplementary Table 4 and Supplementary Text).

In total, we resolved 8,365 rare (as defined by a minor allele frequency [MAF] < 1% across all samples [50% reciprocal overlap]) CNV calls of at least 50 kbps in length and spanning a minimum of 10 probes. We assessed global CNV burden in terms of the number of CNVs, total CNV length, and the number of genes affected by CNVs, stratified by CNV type, size, and frequency. When considering all CNVs, we observed a modest but significant enrichment in TS across all metrics of burden for single-occurrence events (or singletons, corresponding to a MAF of approximately 0.00015) only (OR per CNV of 1.09 [1.01-1.18], p=0.03; OR per 100kb of 1.022 [1.006-1.035], $p=6 \times 10^{-3}$; OR per gene of 1.016 [1.004-1.030], p=0.01; Supplementary Table 5). In general, CNV burden for TS was greater with increasing event size and rarity, with the most substantial effect seen among large singleton deletions (>1 Mb), with an OR per CNV of 2.82 [1.36-6.18], $p=7 \times 10^{-3}$ (Figure 1).

We next evaluated the dataset for possible enrichment of rare CNVs at specific loci, conducting a point-wise (segmental) test of association, treating deletions and duplications independently. As non-overlapping CNVs that affect the same gene would be unaccounted for by segmental assessments of enrichment, we also performed a complementary test collapsed on individual genes conditioned on exonic CNVs affecting protein-coding genes. In contrast to genome-wide association studies of SNPs, there is no generally accepted threshold to indicate genome-wide significance for CNVs. Therefore, for both tests, we established locus-specific (P_{locus}) and genome-wide corrected (P_{corr}) p-values empirically through 1,000,000 permutations, using the max(T) method to control for familywise error rate (FWER)[7]. Both tests converged on the same two distinct loci, one for deletions and another for duplications, which were enriched among TS cases and survived correction for multiple testing.

For deletions, the peak segmental association signal was located at rs13418185 ($P_{locus}=6 \times 10^{-6}$, $P_{corr}=8.6 \times 10^{-4}$, Figure 2a), corresponding to heterozygous losses across the first three exons of *NRXN1*, found exclusively among TS cases (N=10, Figure 2a and b). In the gene-based test of genome-wide exonic CNVs, *NRXN1* deletions were the most significant association (Supplementary Table 6 and Supplementary Figure 6), representing 12 cases (0.49%) and a single control (0.02%); OR=20.3 [2.6-156.2]; $P_{locus}=6.2 \times 10^{-5}$; $P_{corr}=6.7 \times 10^{-4}$. Consistent with deletions previously identified for this gene in ASD, SCZ, and epilepsy, these exon-spanning CNVs clustered at the 5' end of the gene and predominantly affected the α isoform of *NRXN1*[8].

The most significant segmental association with a duplication was located within the *CNTN6* gene at rs4085434 ($P_{locus}=3.7 \times 10^{-5}$, $P_{corr}=6.5 \times 10^{-3}$) with a secondary peak located directly upstream ($P_{locus}=5.4 \times 10^{-5}$, $P_{corr}=6.5 \times 10^{-3}$, Figure 2a and c). Closer inspection of the locus revealed an enrichment of large duplications spanning this gene. A gene-based test determined that duplications overlapping *CNTN6* correspond to an OR=10.1 [2.3-45.4] for TS ($P_{locus}=2.5 \times 10^{-4}$, $P_{corr}=8.3 \times 10^{-3}$), with gains found in 12 cases (0.49%) and 2 controls (0.05%) (Supplementary Table 6 and Supplementary Figure 7). All duplications detected across *CNTN6* were heterozygous and spanned exons.

No other loci were significant after controlling for FWER, under either segmental or gene-based tests of association. We obtained similar results after pair-matching each individual case with its closest ancestrally matched control, demonstrating that these results are robust and not the result of inter-European population stratification or case-control sample biases (Supplementary Text and Supplementary Figure 8). Furthermore, we observed no significant enrichment of any CNVs among controls.

Excluding these two genome-wide significant loci, we conducted a secondary analysis testing for an increased burden among 27 rare, recurrent CNVs previously associated with various neurodevelopmental/neuropsychiatric disorders. We observed no nominally significant enrichment, either considering these CNVs individually (Supplementary Table 7) or in concert (P=1.0, 2-sided Fisher's exact test).

Although previous studies have reported heterozygous exonic *NRXN1* deletions in 4 TS patients[9,10], the small sample sizes in these prior studies precluded any definitive association of this deletion with TS. Here, we demonstrate that exonic deletions affecting *NRXN1*, particularly those spanning exons 1-3, confer a substantial increase in risk for the disorder. Of note, among the 12 TS cases with exonic *NRXN1* deletions, four had another previously diagnosed neurodevelopmental disorder (NDD), including two with ASD (Supplementary Table 8). The association of *NRXN1* deletions with different neurodevelopmental disorders represents one of the most consistent findings regarding CNVs in neuropsychiatry[8,11,12]. Our data suggests an approximately two-fold higher prevalence of exonic *NRXN1* deletions in TS compared to other neuropsychiatric disorders[12], although much larger replication cohorts will be necessary to affirm this apparent comparative enrichment. Despite the diverse clinical presentation exhibited by *NRXN1* deletion carriers, *in vitro* models using human neurons differentiated from induced pluripotent stem cells have shown independent lines carrying different exonic deletions in the *NRXN1*-α isoform exhibit markedly similar defects in synaptic transmission[13]. NRXN1-α interactions are also critical for thalamocortical synaptogenesis and plasticity[14], underscoring a potential mechanism for its repeated association to developmental neuropsychiatric disorders.

Like *NRXN1*, *CNTN6* encodes a cell-adhesion molecule that has been shown to promote neurite outgrowth. On the basis of structural variation, *CNTN6* has been proposed as a candidate gene for intellectual disability and/or developmental delay[15,16], and deletions affecting *CNTN6* are significantly enriched in ASD[17]. However, none of the subjects with *CNTN6* duplications identified here had a known NDD (Supplementary Table 8). Notably, the *CNTN6* duplications identified in our sample are considerably larger in TS cases compared to controls (641.0 vs. 142.9 kbp). 9 out of 12 TS carriers harbor a duplication exceeding 500 kbp in length, while both of the *CNTN6* duplications found in controls were less than 200 kbp. Furthermore, in a previous CNV study of 1,086 TS cases and 1,789 controls unrelated to the samples used in the current analysis, duplications directly upstream of *CNTN6* demonstrated the greatest enrichment[18], reinforcing a possible pathogenic significance of *CNTN6* duplications to this disorder. Consistent with northern blot analysis in the adult human nervous system[19], examination of human brain RNAseq data from the BrainSpan project indicates that *CNTN6* is widely expressed postnatally with highest expression seen both prenatally and postnatally in the cerebellum and mediodorsal thalamus, with additional focal expression in mid-gestational frontal and sensorimotor cortex (Supplementary Figure 9). The thalamus has long been a region of proposed involvement in TS based on multiple levels of evidence including thalamic lesions, human neurophysiology studies, and by recent treatments successes using deep-brain stimulation[20,21]. The cerebellum has also recently been implicated in TS by functional magnetic resonance imaging[22].

In summary, we have conducted the largest survey of structural variation in TS to date. We identified two genome-wide significant loci that are enriched for rare CNVs in TS: deletions in *NRXN1* and duplications in *CNTN6*. Approximately 1% of TS cases carry a CNV in either gene. Furthermore, we demonstrate a significant increase in global CNV burden, primarily for large, extremely rare deletions. This result suggests that additional CNVs that confer susceptibility to TS remain, but their discovery will likely require substantial increases in sample size.

Summarized Methods

Sample ascertainment and data generation

TS cases were ascertained through 21 sites across North America, Europe, and Israel through either specialty clinics or a web-based recruitment effort using a validated diagnostic instrument (TICS Inventory, Supplementary Text). A definite DSM-IV-TR diagnosis of TS, determined by an expert clinician, was a requisite for study inclusion. Unselected control samples were collected in conjunction with TS cases. Additional unscreened controls were obtained from four external studies, and SNP data was generated for all samples on the Illumina OmniExpress platform (Supplementary Text and Supplementary Table 1) according to the manufacturer's specifications. Raw intensities were obtained using GenomeStudio (Illumina). Quality Control (QC, Supplementary Text and Supplementary Table 1b) was conducted using PLINK v. 1.90, Perl, and R scripts. Samples were further excluded if they were of discrepant or indeterminate genetic sex or were outliers based on heterozygosity (Supplementary Figure 2a). When samples exhibited an excessive amount of cryptic relatedness (PI-HAT > 0.185), only the sample with the higher call rate was retained. In addition, control samples that exhibited an excessive amount of cryptic relatedness to individuals clinically diagnosed with a neuropsychiatric phenotype were also removed.

Ancestry inference and matching

Genotype data was combined with data from publicly available HapMap samples of European, African, and Asian continental ancestry (Illumina). All available European (EU) population samples from the 1000 Genomes Project were also included to establish an appropriate calibration threshold for EU ancestry designation. A total of 19,024 LD-independent markers were used for ancestry inference, and samples were excluded if they contained > 0.0985 non-EU ancestry as determined using fastStructure (Supplementary Figure 2).

CNV calling

Only SNP assays common to all versions of the OmniExpress arrays were used for CNV detection (n=689,077) to mitigate any disparity in CNV detection due to probe coverage. Raw CNV calls were generated on all autosomal chromosomes using PennCNV and QuantiSNP. In addition to hard cutoffs used to flag problematic assays, samples were excluded if they represented outliers in a number of CNV quality metrics (determined as mean ±3 SD or by manual inspection, Supplementary Figure 1). Rare CNVs, defined by a prevalence of <1% across all samples, were validated with an alternative locus specific CNV genotyping algorithm that considers normalized, median-summarized intensity values across each putative CNV region. An overview of the CNV processing pipeline is presented in Supplementary Figure 1 and described in detail in the Supplementary Text.

Burden analysis of global CNV burden

Under a logistic regression model, we assessed for global CNV burden as measured by the total number of CNVs, cumulative CNV length, or number of genes spanned by CNVs, including covariates found to be significantly associated with these burden metrics (Supplementary Text and Supplementary Table 9). Odds ratios indicate an increase in risk for TS per unit of CNV burden. P-values were calculated using the likelihood ratio test.

Locus-specific tests of association

The segmental test of association was performed at all unique CNV breakpoints. For gene-based association tests, we considered only CNVs spanning exons of coding genes as defined by Refseq annotation. Significance for both tests of association was determined by 1,000,000 permutations of phenotype labels. In each case, both locus-specific and genome-wide corrected p-values were obtained using the max(T) permutation method as implemented in PLINK v1.07, which controls for family-wise error rate by comparing the locus-specific test statistic to all test statistics genome-wide within each permutation.

Analysis of known neuropsychiatric susceptibility loci

A list of known CNVs with strong evidence of association to various neuropsychiatric disorders, including ASD, ID/DD, SCZ, and BD was assembled from the literature[4]. For recombination hotspots, a CNV was counted if it overlapped with the reported region by at least 50%. Single-gene associated CNVs were considered if they shared overlap to annotated gene boundaries as annotated in RefSeq. Locus-specific P-values were determined by 100,000 permutations of phenotype labels.

URLs

PennCNV, http://penncnv.openbioinformatics.org; QuantiSNP, https://sites.google.com/site/quantisnp/home; HapMap3, ftp://ftp.ncbi.nlm.nih.gov/hapmap; 1000 Genomes Project; http://www.1000genomes.org; BrainSpan, http://www.brainspan.org

ACKNOWLEDGMENTS

The authors wish to thank all the patients with Tourette Syndrome and their families, as well as unaffected volunteers, who generously agreed to participate in this study. This study was supported by the US National Institutes of Health U01 NS040024 to Drs. Pauls, Mathews, and Scharf and the Tourette Syndrome Association International Consortium for Genetics, ARRA Grant NS040024-09S1, K23 MH085057, and K02 NS085048 to Dr. Scharf, ARRA Grants NS040024-07S1 and NS016648 to Dr. Pauls, MH096767 to Dr. Mathews and NINDS Informatics Center for Neurogenetics and Neurogenomics grant P30 NS062691 to Drs. Coppola and Freimer, by grants from the Tourette Association of America to Drs. Paschou, Pauls, Mathews, and Scharf and from the German Research Society to Dr. Hebebrand.

AUTHOR CONTRIBUTIONS

All authors were involved in the conception and design of the genetic study. A.H., P.P., C.A.M., J.M.S., and G.C. designed and oversaw the analyses. A.H., D.Y., L.K.D., J.H.S., F.T., V.R., I.Z., E.M.R., L.O., J.A.C., L.M.M., B.M.N., N.B.F., P.P., C.A.M., J.M.S., and G.C. participated in the conduct of the analyses. Major contributions to writing and editing were made by A.H., C.A.M., J.M.S, and G.C. All authors assisted with critically revising the manuscript.

COMPETING FINANCIAL INTERESTS

The authors declare competing financial interest: details are available in the online version of the paper.

P.S., M.G., H.S.S., R.A.K., Y.D., G.R., C.L.B., G.L., W.M.M., D.L.P, N.J.C., N.B.F., P.P., C.A.M. and J.M.S have received research funding from the Tourette Association of America (TAA). J.M.S., C.A.M. have received travel support from the TAA and serve on the TAA Scientific Advisory Board. J.M.S. has also received consulting fees from Nuvelation Pharma, Inc. P.S.

received unrestricted Educational Grants in support of conferences he organized from Purdue and Shire, a CME speaker fee from Purdue University, industry sponsored clinical trial support from Otsuka and is a member of the Data Safety Monitoring Committee at Psyadon. C.L.B. has received funding for clinical trials from Psyadon Pharmaceuticals, Neurocrine Pharmaceuticals, Synchroneuron Pharmaceuticals, AUSPEX Pharmaceuticals, and TEVA Pharmaceuticals. She was a paid speaker for the TAA CDC program and a paid consultant for Bracket eCOA. I.A.M. has participated in research funded by the National Parkinson Foundation, TAA, Abbvie, Auspex, Biotie, Michael J. Fox Foundation, Neurocrine, Pfizer, and Teva, but has no owner interest in any pharmaceutical company. I.A.M. has been reimbursed for speaking for the National Parkinson Foundation and TAA. M.S.O. serves as a consultant for the National Parkinson Foundation, and has received research grants from NIH, NPF, the Michael J. Fox Foundation, the Parkinson Alliance, Smallwood Foundation, the Bachmann-Strauss Foundation, the TAA, and the UF Foundation. M.S.O's DBS research is supported by: R01 NR014852 and R01NS096008. He has previously received honoraria, but in the past >60 months has received no support from industry. M.S.O. has received royalties for publications with Demos, Manson, Amazon, Smashwords, Books4Patients, and Cambridge, is an associate editor for New England Journal of Medicine Journal Watch Neurology, has participated in CME and educational activities on movement disorders in the last 36 months sponsored by PeerView, Prime, QuantiaMD, WebMD, Medicus, MedNet, Henry Stewart, and by Vanderbilt University. The institution and not M.S.O. receives grants from Medtronic, Abbvie, Allergan, and ANS/St. Jude, and the PI has no financial interest in these grants. D.W.W. has received royalties from Guilford Press and Oxford University Press, speaking honoraria from the TAA and serves on the TAA Medical Advisory Board. All other authors have no competing financial interests to declare.

References

1. Scharf, J. M. *et al.* Population prevalence of Tourette syndrome: a systematic review and meta-analysis. *Mov. Disord.* **30,** 221–228 (2015).
2. Mataix-Cols, D. *et al.* Familial Risks of Tourette Syndrome and Chronic Tic Disorders. A Population-Based Cohort Study. *JAMA Psychiatry* **72,** 787–793 (2015).
3. Davis, L. K. *et al.* Partitioning the heritability of Tourette syndrome and obsessive compulsive disorder reveals differences in genetic architecture. *PLoS Genet.* **9,** e1003864 (2013).
4. Malhotra, D. & Sebat, J. CNVs: harbingers of a rare variant revolution in psychiatric genetics. *Cell* **148,** 1223–1241 (2012).
5. Wang, K. *et al.* PennCNV: an integrated hidden Markov model designed for high-resolution copy number variation detection in whole-genome SNP genotyping data. *Genome Res.* **17,** 1665–1674 (2007).
6. Colella, S. *et al.* QuantiSNP: an Objective Bayes Hidden-Markov Model to detect and accurately map copy number variation using SNP genotyping data. *Nucleic Acids Res.* **35,** 2013–2025 (2007).
7. Westfall, P. H. & Troendle, J. F. Multiple testing with minimal assumptions. *Biom. J.* **50,** 745–755 (2008).
8. Ching, M. S. L. *et al.* Deletions of NRXN1 (neurexin-1) predispose to a wide spectrum of developmental disorders. *Am. J. Med. Genet. B Neuropsychiatr. Genet.* **153B,** 937–947 (2010).
9. Sundaram, S. K., Huq, A. M., Wilson, B. J. & Chugani, H. T. Tourette syndrome is associated with recurrent exonic copy number variants. *Neurology* **74,** 1583–1590 (2010).
10. Nag, A. *et al.* CNV analysis in Tourette syndrome implicates large genomic rearrangements in COL8A1 and NRXN1. *PLoS One* **8,** e59061 (2013).
11. Glessner, J. T. *et al.* Autism genome-wide copy number variation reveals ubiquitin and neuronal genes. *Nature* **459,** 569–573 (2009).
12. Rujescu, D. *et al.* Disruption of the neurexin 1 gene is associated with schizophrenia. *Hum. Mol. Genet.* **18,** 988–996 (2009).
13. Pak, C. *et al.* Human Neuropsychiatric Disease Modeling using Conditional Deletion Reveals Synaptic Transmission Defects Caused by Heterozygous Mutations in NRXN1. *Cell Stem Cell* **17,** 316–328 (2015).
14. Singh, S. K. *et al.* Astrocytes Assemble Thalamocortical Synapses by Bridging NRX1α and NL1 via Hevin. *Cell* **164,** 183–196 (2016).

15. Hu, J. *et al.* CNTN6 copy number variations in 14 patients: a possible candidate gene for neurodevelopmental and neuropsychiatric disorders. *J. Neurodev. Disord.* **7,** 26 (2015).
16. Kashevarova, A. A. *et al.* Single gene microdeletions and microduplication of 3p26.3 in three unrelated families: CNTN6 as a new candidate gene for intellectual disability. *Mol. Cytogenet.* **7,** 97 (2014).
17. Mercati, O. *et al.* CNTN6 mutations are risk factors for abnormal auditory sensory perception in autism spectrum disorders. *Mol. Psychiatry* (2016). doi:10.1038/mp.2016.61
18. McGrath, L. M. *et al.* Copy number variation in obsessive-compulsive disorder and tourette syndrome: a cross-disorder study. *J. Am. Acad. Child Adolesc. Psychiatry* **53,** 910–919 (2014).
19. Kamei, Y., Tsutsumi, O., Taketani, Y. & Watanabe, K. cDNA cloning and chromosomal localization of neural adhesion molecule NB-3 in human. *J. Neurosci. Res.* **51,** 275–283 (1998).
20. Hassler, R. & Dieckmann, G. [Stereotaxic treatment of tics and inarticulate cries or coprolalia considered as motor obsessional phenomena in Gilles de la Tourette's disease]. *Rev. Neurol.* **123,** 89–100 (1970).
21. Gunduz, A. *et al.* Proceedings of the Second Annual Deep Brain Stimulation Think Tank: What's in the Pipeline. *Int. J. Neurosci.* **125,** 475–485 (2015).
22. Bohlhalter, S. *et al.* Neural correlates of tic generation in Tourette syndrome: an event-related functional MRI study. *Brain* **129,** 2029–2037 (2006).

Supplementary Text

Sample Ascertainment

Tourette Syndrome (TS) cases were ascertained primarily from TS specialty clinics through sites distributed throughout North America, Europe and Israel as part of an ongoing collaborative effort by the Tourette Syndrome Association International Consortium for Genetics (TSAICG) as described in detail elsewhere[23]. Subjects were assessed for a lifetime diagnosis of TS, Obsessive Compulsive Disorder (OCD) and Attention-Deficit/Hyperactivity Disorder (ADHD) using a standardized and validated semi-structured direct interview (TICS Inventory[24,25]). An additional 628 cases were collected at 9 TS specialty clinics in Austria, Canada, France, Germany, Greece, Hungary, Italy and the Netherlands by expert clinicians using Tourette Syndrome Study Group criteria for Definite TS (DSM-IV TS diagnosis plus tics observed by a trained clinician) as well as DSM-IV diagnostic criteria for OCD and ADHD, along with 610 ancestry-matched controls as described previously[26]. Formal standardized assessments were not conducted for other neurodevelopmental disorders (NDDs) such as Intellectual Disability/Developmental Delay (ID/DD), Autism Spectrum Disorder (ASD), or schizophrenia/childhood psychosis; however, participants and their parents were asked about the presence of established or suspected NDD diagnoses.

Lastly, in an effort to greatly increase sample size for TS genetic studies in a cost-effective manner, additional TS case samples were obtained through web-based recruitment of individuals with a prior clinical diagnosis of TS who subsequently completed an online questionnaire that we have validated against the gold-standard TS structured diagnostic interview with nearly 100% concordance for all inclusion/exclusion criteria as well as high correct classification rates for DSM-IV diagnoses of OCD and ADHD[25,27]. Individuals for web-based screening were solicited through the Tourette Association of America mailing list as well as from 4 TS specialty clinics in the United States. Individuals with a history of intellectual disability, seizure disorder, or a known tic disorder unrelated to TS were excluded.

Additional control subjects were taken from four external large-scale genetic studies consisting of healthy individuals sampled from similar geographic locations and genotyped on the same Illumina OmniExpress platform as the TS cases:

1) Cardiff Controls (CC): UK Blood donors were recruited in Cardiff at the time of blood donation at centers in Wales and England. Although not explicitly screened for psychiatric disorders, these controls are likely to have low rates of severe neuropsychiatric illness, as blood

donors in the UK are only eligible to donate if they are not taking any medications. 57% of these controls were male.

2) Consortium for Neuropsychiatric Phenomics (CNP): A collection of neuropsychiatric samples composed of patients with attention deficit hyperactivity disorder (ADHD), bipolar disorder (BD), schizophrenia (SCZ), and psychologically normal controls, collected throughout North America as part of a large NIH Roadmap interdisciplinary research consortia centered at the University of California, Los Angeles. Only the control samples were used in this study.

3) Genomic Psychiatry Cohort (GPC)[28]: A large, longitudinal, population resource composed of clinically ascertained patients affected with BD, SCZ, their unaffected family members, and a large set of control samples with no family history of either disorder. Samples were collected at various sites throughout North America in a National Institute of Mental Health-sponsored study lead by the University of Southern California.

4) Welcome Trust Case Control Consortium 2 (WTCCC2)[29]: Selected control samples from the National Blood Donors Cohort.

Genotyping and data processing

Cases and controls collected specifically for this study were all genotyped on the Illumina OmniExpress Exome v1.1, while the remaining control samples from the CC, CNP, GPC, and WTCCC2 cohorts were genotyped on the Illumina OmniExpress 12v1.0. The content of these two arrays is identical except for 1) exome-focused content on the former and 2) additional intensity-only markers on the latter. We have observed that exome-specific assays in general exhibit a much higher variance overall in their derived log-R ratio (LRR). Therefore, in order to avoid detection biases due to this differential variance, as well as from unequal probe coverage, only the SNP assays common to all versions of the OmniExpress arrays in this study were used for quality control (QC) and CNV detection, a total of 689,077 markers.

To ensure the generation of the most reliable SNP calls, intensity measures, and B-allele frequencies (BAF), as well as to reduce the effect of differential processing, a custom cluster file was generated for each individual genotyping batch. Since the performance of Illumina's proprietary normalization and cluster generation process is dependent on the number of samples, we processed all of the raw data, regardless of phenotype, with subsequent removal of clinical samples from the CNP and GPC datasets prior to analysis. An initial round of quality control (QC) was carried out using Illumina Beeline to determine baseline calling rates for each sample using the canonical cluster file (*.egt) provided by the manufacturer for each array version. Any sample with a call rate < 0.98 or a log-R ratio (LRR) standard deviation > 0.30 was deemed a failed assay and removed (Pre-cluster QC, Supplementary Table 1). SNP clustering was then performed in GenomeStudio with only passing samples within each genotyping batch. This process was repeated for all datasets.

Genome-wide detection of CNV loci

We employed two widely-used HMM-based CNV calling algorithms, PennCNV (version 2011-05-03) and QuantiSNP (version 2.0), to initially detect structural variants in our dataset. We created GC-adjusted LRR intensity files for all samples using the GC-waviness correction method described by Diskin et al[30]. For PennCNV, a custom population B-allele frequency file was created for each genotyping batch separately and CNV calls were generated using the standard protocol. QuantiSNP calls were generated on the GC-adjusted intensity files. A concordant callset between both CNV callers was then generated by taking the intersecting boundaries of overlapping calls of the same CNV type (deletion or duplication). Additionally, adjacent CNV calls were merged if they were spanned by a CNV called by the other HMM algorithm. As HMMs have been shown to artificially break up large CNVs, we also merged CNV segments in the final concordant callset if they were of the same copy number and the number of intervening markers between them was less than 20% of the total of both segments combined. We repeated this process iteratively until no more joining occurred.

Sensitivity assessment

Since the samples in this study were consolidated from multiple studies, subtle differences in the ability to detect genetic variation between cases and controls could lead to spurious associations. This issue is even more critical in studies involving CNVs, given the inherent imprecise nature of their detection.

Therefore, prior to association testing, we augmented a previously described method[7] to investigate whether any difference in sensitivity to detect CNVs existed between cases and controls within the context of our study. Both HMM-based CNV callers we employed for genome-wide detection are univariate methods completely agnostic of intensity information across multiple samples and do not use known population frequency prior probabilities in their calling algorithms. Therefore, common CNVs act as an ideal proxy to evaluate the effectiveness to detect rare events accurately, given that they are detected in the same manner but are present at much higher frequencies.

To facilitate data processing and visualization, we first generated an HDF5 database containing the LogR-Ratio (LRR) intensity and B-allele frequency (BAF) values for all samples. Normalized intensity values across each individual were generated by converting the GC-corrected, median-centered LRR measures into Z-scores. We used the UCSC Genome Browser liftOver tool to translate a list of common HapMap3 CNVs to the hg19 reference. To match the thresholds used for our association tests in this study, we filtered the list of common CNVs to those that were >50 kbp in length. We reduced the number of markers required slightly to a minimum of 9 to ensure that an adequate number of events could be assessed. For each common CNV meeting these criteria, we examined the distribution of median-summarized normalized intensity measures within the CNV region across all study samples and retained only those loci that exhibited discrete clustering into distinct copy-number states. A total of 11 common CNV loci were retained for sensitivity analysis.

We generated locus-specific genotyping calls in the following manner. First, we extracted the LRR intensity Z-scores for all probes in the region across all samples. The Z-scores for all probes spanning the CNV locus were then subjected to a second round of normalization in order to normalize scores across all samples; this was found to aid in the automation of the clustering procedure. A Gaussian mixture model (GMM) was fit to this distribution to cluster samples into discrete CNV groups using the SciKit-learn Python package. The optimum number of clusters was automatically determined by minimization of the Bayesian Information Criterion (BIC) and corrected, when necessary, by manual inspection. Individuals were assigned to a cluster only if the posterior probability of assignment exceeded 0.95.

Copy number state was inferred by examining the original LRR intensity values for samples within each cluster. We inspected for allele frequency differences between controls and cases for all clusters and found no significant difference (Fisher exact test, Supplementary Table 3). We collapsed the clusters at each locus into CNVs of the same type (deletion or duplication). As this locus-specific genotyping method is more sensitive than HMM segmentation methods, we used the proportion of concordant of HMM-based calls as a measure of segmentation detection sensitivity. We found no significant difference in sensitivity to detect common CNVs between phenotypic groups at any of the 11 loci tested, either independently, or in concert (Fisher exact test, Supplementary Tables 4a and 4b). Furthermore, the mean sensitivity for each sample was calculated and collectively assessed for any systematic difference between phenotypic groups. Considering duplications, deletions, or both in concert, we observed no significant difference in the sensitivity of segmentation calls between case and control groups (Welch *t*-test, Supplementary Table 4c), thus validating our preprocessing, QC, and CNV-calling procedures. Results obtained by fitting mixture models separately by either phenotype or batch produced similar results.

Call filtering, delineation of rare events, and in-silico validation

Calls were removed from the dataset if they spanned less than 10 markers, were less than 50kb in length, or overlapped by more than 0.5 of their total length with regions known to generate artifacts in SNP-based detection of CNVs, including immunoglobulin, telomeric (defined as 100kb from the chromosome ends) and centromeric regions, segmental duplications, and regions that have previously demonstrated associations specific to Epstein-Barr virus immortalized cell lines[29]. We filtered our callset for rare CNVs, defined as those events with MAF approximately < 1% (no more than 65 occurrences across 6,435 samples), based on a reciprocal overlap of 50% with CNVs of the same copy-number state. As the number of rare CNVs in a cohort such as ours is exceedingly large, traditional methods that rely on manual inspection of all putative CNV calls constitutes an approach that is both inconsistent and impractical. Therefore, for each putative rare CNV, we generated two different metrics based on intensity (LRR-Z) and BAF banding (BAF_{del} and BAF_{dup}), and calculated population frequency estimates (OUTLIER-Z) by inspecting the distribution of intensities across the entire sample (Supplementary Figure 4a).

For qualifying CNVs based on intensity, we adopted a scoring methodology similar to the MeZOD method described previously[32,33], with a noted exception. We observed that standardized intensity measures from Illumina data typically range from < -20 for homozygous deletions, [-6,-2.5] for heterozygous deletions, and > 1.5 for duplications. Because of the disproportionately large effect on intensity measures caused by deletion events, performing a second round of normalization across all samples within each putative CNV often skews the overall distribution when such events are present. Therefore, we only performed a single round of normalization of LRR intensity measures within each sample. Each CNV is scored by calculating the median of LRR intensity Z-scores (LRR-Z) for all probes within the region. To determine reasonable thresholds for intensity metrics specific to our Omniexpress assay, we applied our CNV calling pipeline on 266 HapMap samples genotyped on the same OmniExpress platform, provided by Illumina. We compared these HapMap calls to those generated using high-coverage array comparative genome hybridization (aCGH)[34]. 11 samples overlapped between these two datasets. For these individuals, we extracted the LRR-Z for all aCGH-validated CNV calls and inspected the distribution of all calls for both deletions and duplications in order to establish reasonable, conservative thresholds based on validated CNVs; in this case we required an LRR-Z of <-2.3 for deletions and >+1.3 for duplications (Supplementary Figure 4b).

The BAF banding pattern is particularly informative for the detection of CNV events using SNP arrays. This is particularly true for duplications, as intensity gains are typically modest for these types of events. We calculated the proportion of probes within the CNV region that showed evidence of a deletion (BAF of <0.15 or >0.85) or duplication event (BAF of [0.25-04] or [0.6-0.8]), and denoted these measures "$\mathrm{BAF}_{\mathrm{del}}$" and "$\mathrm{BAF}_{\mathrm{dup}}$". Based on prior observations[35] and from examination of our own data, we conservatively required deletions to have $\mathrm{BAF}_{\mathrm{del}} > 0.9$, and duplications to have a $\mathrm{BAF}_{\mathrm{dup}} > 0.15$.

Furthermore, the distribution of summarized intensity information across all individuals for every putative rare CNV was screened for calling sensitivity by inspecting the distribution of intensities at the locus across all samples. For each rare CNV, we flagged those where the proportion of samples whose LRR-Z metric fell outside of [-2.3, 1.3] (denoted as OUTLIER-Z) and further inspected these regions manually. Putatively rare CNV loci that showed substantial evidence for extensive polymorphism were subsequently scored using the GMM genotyping method described above.

We opted not to impose any hard cutoff for CNV calls with regard to any of these measures to avoid any bias imposed by differential missingness derived from subtle systematic differences between genotyping batches. Rather, these thresholds were applied to flag those CNV calls with marginal scores for manual inspection and filter out only obviously misclassified events. Through this *in silico* validation process, we discovered multiple instances of large copy-number aberrations likely due to individual mosaicism (Supplementary Figure 4c), and two common polymorphic duplication regions misclassified as a rare CNV due to reduced sensitivity of the HMM segmentation (Supplementary Figure 4d). Out of 8,452 initial consensus HMM calls, a total of 87 CNV events were removed. Six of these were due to mosaic events, and the remainder was excluded due to the misclassification of common CNVs as a rare events.

Genome-wide burden analysis

For comparison of genome-wide burden between TS cases and controls, we limited our consideration to rare CNVs spanning a minimum of 10 SNPs and > 50kb in length. We assessed genome-wide CNV burden in three different ways: (1) number of rare CNVs, (2) total CNV length (per 100 KB), and (3) the total number of genes intersected by CNVs. Furthermore, we stratified each test by both size (all CNVs, >500kb, and >1Mb) as well as frequency (rare CNVs and singletons). Frequency counts were determined using PLINK `--cnv-freq-method2 0.5`. Here, singletons are defined as sharing no more than a 50% overlap with any other CNV. Gene overlaps were counted if the CNV overlapped any gene boundary as delineated by Refseq. To examine the effect of different covariates on our different metrics of global CNV burden, we first fit a linear regression model for each type of burden test:

$$Burden\_metric \sim genotyping\_batch + subject\_sex + LRR\_SD + ancestry\_PCs$$

None of the included covariates, which included the top 10 ancestry PCs, were significant predictors of global CNV burden as measured by either total number of CNVs or cumulative CNV length (Supplementary Table 6a). Separately, we examined the effect of these covariates exclusively with regard to the burden due to small CNV events, as these are most likely affected by minor fluctuations in assay quality and subtle differences in sample ascertainment. We found that LRR_SD was significantly associated with small CNV burden (defined here as CNVs < 100kb in length) for both total CNV number and CNV size (Supplementary Table 6b and 6c), and was therefore included in the burden analysis as a covariate.

To assess for a global burden difference between TS and controls, we fit a logistic regression model in R with affectation status as the dependent variable and the burden metric and LRR_SD as independent variables. ORs indicate an increase in risk for TS as assessed per CNV, per 100kb of total CNV length, or per gene affected by CNVs. P-values were calculated using the likelihood ratio test.

Validation of association results

We repeated the segmental association test after carefully pair-matching each case with a control such that the global difference between each pair was minimized using SpectralGEM[32] (Supplementary Figure 8). For the matched segmental association analysis, because of the drastic reduction in sample size, a corrected p-value < 0.05 was used as a cutoff to indicate genome-wide significance.

Supplementary references

23. Scharf, J. M. *et al.* Genome-wide association study of Tourette's syndrome. *Mol. Psychiatry* **18,** 721–728 (2013).
24. Tourette Syndrome Association International Consortium for Genetics. Genome scan for Tourette disorder in affected-sibling-pair and multigenerational families. *Am. J. Hum. Genet.* **80,** 265–272 (2007).
25. Darrow, S. M. *et al.* Web-based phenotyping for Tourette Syndrome: Reliability of common co-morbid diagnoses. *Psychiatry Res.* **228,** 816–825 (2015).
26. Paschou, P. *et al.* Genetic association signal near NTN4 in Tourette syndrome. *Ann. Neurol.* **76,** 310–315 (2014).
27. Egan, C. A. *et al.* Effectiveness of a web-based protocol for the screening and phenotyping of individuals with Tourette syndrome for genetic studies. *Am. J. Med. Genet. B Neuropsychiatr. Genet.* **159B,** 987–996 (2012).
28. Pato, M. T. *et al.* The genomic psychiatry cohort: partners in discovery. *Am. J. Med. Genet. B Neuropsychiatr. Genet.* **162B,** 306–312 (2013).
29. Power, C. & Elliott, J. Cohort profile: 1958 British birth cohort (National Child Development Study). *Int. J. Epidemiol.* **35,** 34–41 (2006).
30. Diskin, S. J. *et al.* Adjustment of genomic waves in signal intensities from whole-genome SNP genotyping platforms. *Nucleic Acids Res.* **36,** e126 (2008).
31. Shirley, M. D. *et al.* Chromosomal variation in lymphoblastoid cell lines. *Hum. Mutat.* **33,** 1075–1086 (2012).
32. Kirov, G. *et al.* De novo CNV analysis implicates specific abnormalities of postsynaptic signalling complexes in the pathogenesis of schizophrenia. *Mol. Psychiatry* **17,** 142–153 (2012).
33. McCarthy, S. E. *et al.* Microduplications of 16p11.2 are associated with schizophrenia. *Nat. Genet.* **41,** 1223–1227 (2009).
34. Conrad, D. F. *et al.* Origins and functional impact of copy number variation in the human genome. *Nature* **464,** 704–712 (2010).
35. Sanders, S. J. *et al.* Insights into Autism Spectrum Disorder Genomic Architecture and Biology from 71 Risk Loci. *Neuron* **87,** 1215–1233 (2015).
36. Lee, A. B., Luca, D., Klei, L., Devlin, B. & Roeder, K. Discovering genetic ancestry using spectral graph theory. *Genet. Epidemiol.* **34,** 51–59 (2010).
37. Vacic, V. *et al.* Duplications of the neuropeptide receptor gene VIPR2 confer significant risk for schizophrenia. *Nature* **471,** 499–503 (2011).

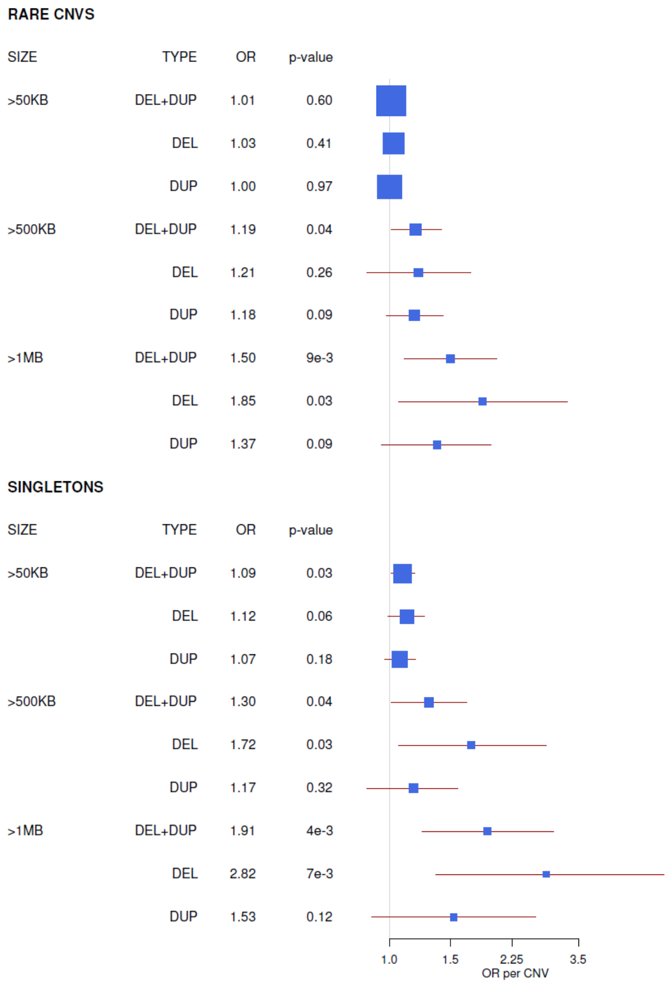

RARE CNVS

SIZE	TYPE	OR	p-value
>50KB	DEL+DUP	1.01	0.60
	DEL	1.03	0.41
	DUP	1.00	0.97
>500KB	DEL+DUP	1.19	0.04
	DEL	1.21	0.26
	DUP	1.18	0.09
>1MB	DEL+DUP	1.50	9e-3
	DEL	1.85	0.03
	DUP	1.37	0.09

SINGLETONS

SIZE	TYPE	OR	p-value
>50KB	DEL+DUP	1.09	0.03
	DEL	1.12	0.06
	DUP	1.07	0.18
>500KB	DEL+DUP	1.30	0.04
	DEL	1.72	0.03
	DUP	1.17	0.32
>1MB	DEL+DUP	1.91	4e-3
	DEL	2.82	7e-3
	DUP	1.53	0.12

Figure 1. Global CNV burden in Tourette Syndrome (TS) increases with both size and rarity of events. Forest plots show OR and 95% CI estimates for an increased risk for TS per CNV, determined by fitting a logistic regression model of phenotype status against CNV count with significant covariates (Supplementary methods). All CNVs considered are >50kb in length and span a minimum of 10 probes. Rare CNVs denote events with a MAF < 0.01; singletons occur only once in either a case or control, corresponding to a MAF of approximately 0.00015 in this study. P-values are calculated using the likelihood ratio test. Box sizes are proportional to precision.

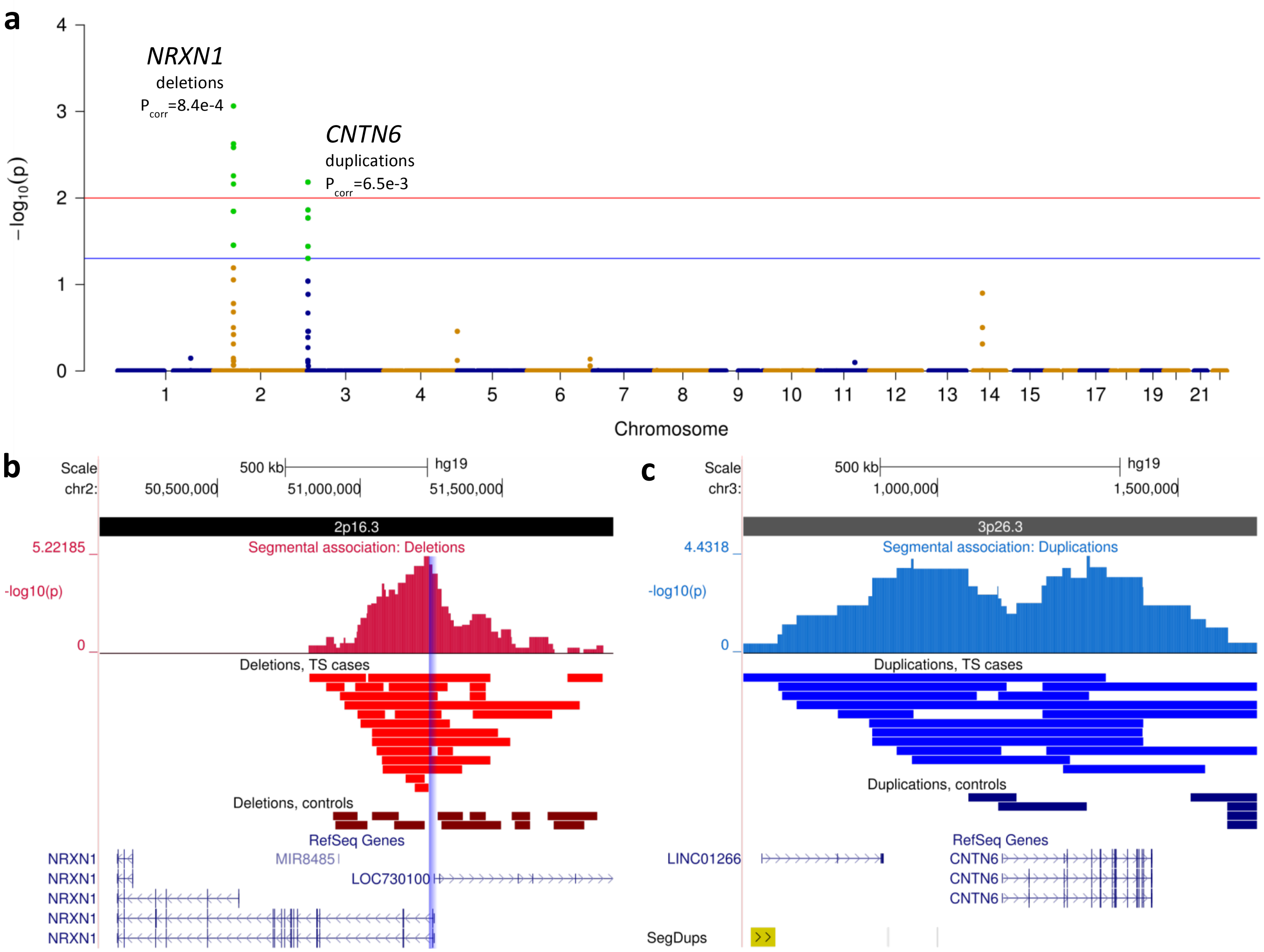

Figure 2. Significant loci enriched for CNVs in TS. (a) Manhattan plot of the results from segmental association tests reveal two genome-wide significant loci: deletions at *NRXN1* and duplications at *CNTN6*. Association tests were conducted separately for gains and losses; for clarity, p-values displayed are empirically corrected for FWER genome-wide using the max(T) method with 1,000,000 permutations and plotted together here. Significance levels representing an α of 0.05 and 0.01 are depicted by blue and red lines, respectively. (b) Heterozygous deletions show a peak of segmental association near the 5' end of *NRXN1* ($p=6.0 \times 10^{-6}$). Deletions spanning the first three exons are found in 10 cases and no controls (blue-shaded bar). Deletions affecting any exon (Supplementary Figure 6) were found in 12 cases (0.49%) and 1 control (0.03%), corresponding to an OR=20.3, 95% CI (2.6-156.2). (c) Structural variation at the *CNTN6* locus. For duplications, the peak of segmental association was located within the *CNTN6* gene ($p=3.7 \times 10^{-5}$). Duplications overlapping this gene correspond to an OR=10.1, 95% CI (2.3-45.4), with heterozygous gains found in 12 cases (0.49%) and 2 controls (0.05%). CNVs overlapping *CNTN6* are considerably larger in cases compared to controls (640.0 vs. 142.9 kb, on average).

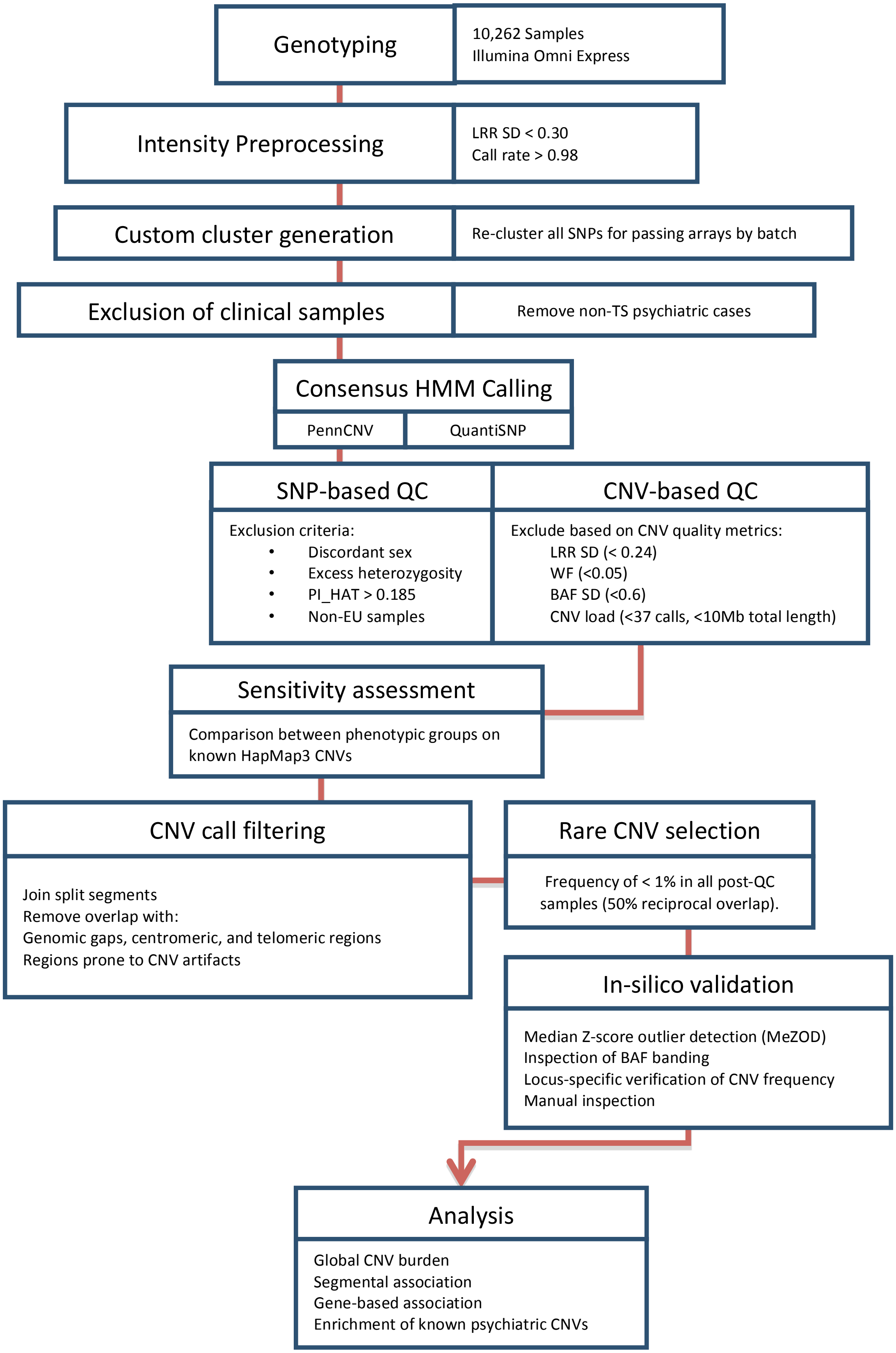
Genotyping
10,262 Samples
Illumina Omni Express
Intensity Preprocessing
LRR SD < 0.30
Call rate > 0.98
Custom cluster generation
Re-cluster all SNPs for passing arrays by batch
Exclusion of clinical samples
Remove non-TS psychiatric cases
Consensus HMM Calling
PennCNV
QuantiSNP
SNP-based QC
Exclusion criteria:
• Discordant sex
• Excess heterozygosity
• PI_HAT > 0.185
• Non-EU samples
CNV-based QC
Exclude based on CNV quality metrics:
LRR SD (< 0.24)
WF (<0.05)
BAF SD (<0.6)
CNV load (<37 calls, <10Mb total length)
Sensitivity assessment
Comparison between phenotypic groups on known HapMap3 CNVs
CNV call filtering
Join split segments
Remove overlap with:
Genomic gaps, centromeric, and telomeric regions
Regions prone to CNV artifacts
Rare CNV selection
Frequency of < 1% in all post-QC samples (50% reciprocal overlap).
In-silico validation
Median Z-score outlier detection (MeZOD)
Inspection of BAF banding
Locus-specific verification of CNV frequency
Manual inspection
Analysis
Global CNV burden
Segmental association
Gene-based association
Enrichment of known psychiatric CNVs

Supplementary Figure 1. Overview of the CNV calling pipeline and analysis. A schematic of the data processing, CNV calling, and analysis is presented here, and described in detail in the supplementary text.

Supplementary Table 1a: Studies and genotyping			
GENOTYPING BATCH	ARRAY	CENTER	PHENOTYPES
CC	OmniExpress v 1.0	Cardiff	Control
CNP	OmniExpress v 1.0	Broad	Control/Clinical
GPC	OmniExpress v 1.0	Broad	Control/Clinical
WTCCC2	OmniExpress v 1.0	Cardiff	Control
TS1	OmniExpress Exome v 1.1	UCLA	Control/TS
TS2	OmniExpress Exome v 1.1	UCLA	Control/TS
TS3	OmniExpress Exome v 1.1	UCLA	Control/TS

Supplementary Table 1b: QC summary								
QC STEP	CC	CNP	GPC	WTCCC2	TS1	TS2	TS3	TOTALS
Initial Samples	1,146	1,511	3,197	960	1,152	2,160	136	10,262
Pre-cluster QC	1,141	1,510	3,126	870	1,148	2,152	135	10,082
Duplicate/Control Samples	1,141	1,491	3,081	870	1,134	2,143	134	9,994
Clinical Phenotype	1,141	1,312	1,388	870	1,134	2,143	134	8,122
Sex Concordance	1,141	1,312	1,387	870	1,132	2,140	134	8,116
Heterozygosity	1,122	1,247	1,301	859	1,107	2,089	133	7,858
Cryptic Relatedness	1,084	1,222	1,264	852	1,100	2,067	132	7,621
CNV/Intensity QC	991	1,106	1,164	832	1,014	1,843	119	6,928
EU Ancestry	959	572	1,143	813	959	1,803	116	6,535

Supplementary Table 1. (a) Summary of included studies and genotyping information. Sample phenotypes, genotyping platform, and genotyping center for different datasets collected for this study are shown, separated by study. (b) Summary of quality control procedures by study. The number of samples remaining within each batch after each successive quality control step (as described in the Supplementary Text) is shown. Study abbreviations: Cardiff Controls (CC), Consortium for Neuropsychiatric Phenomics (CNP), Genomic Psychiatry Cohort (GPC), Wellcome Trust Case-Control Consortium (WTCCC2) and TS cases and controls collected for this study (TS1-3).

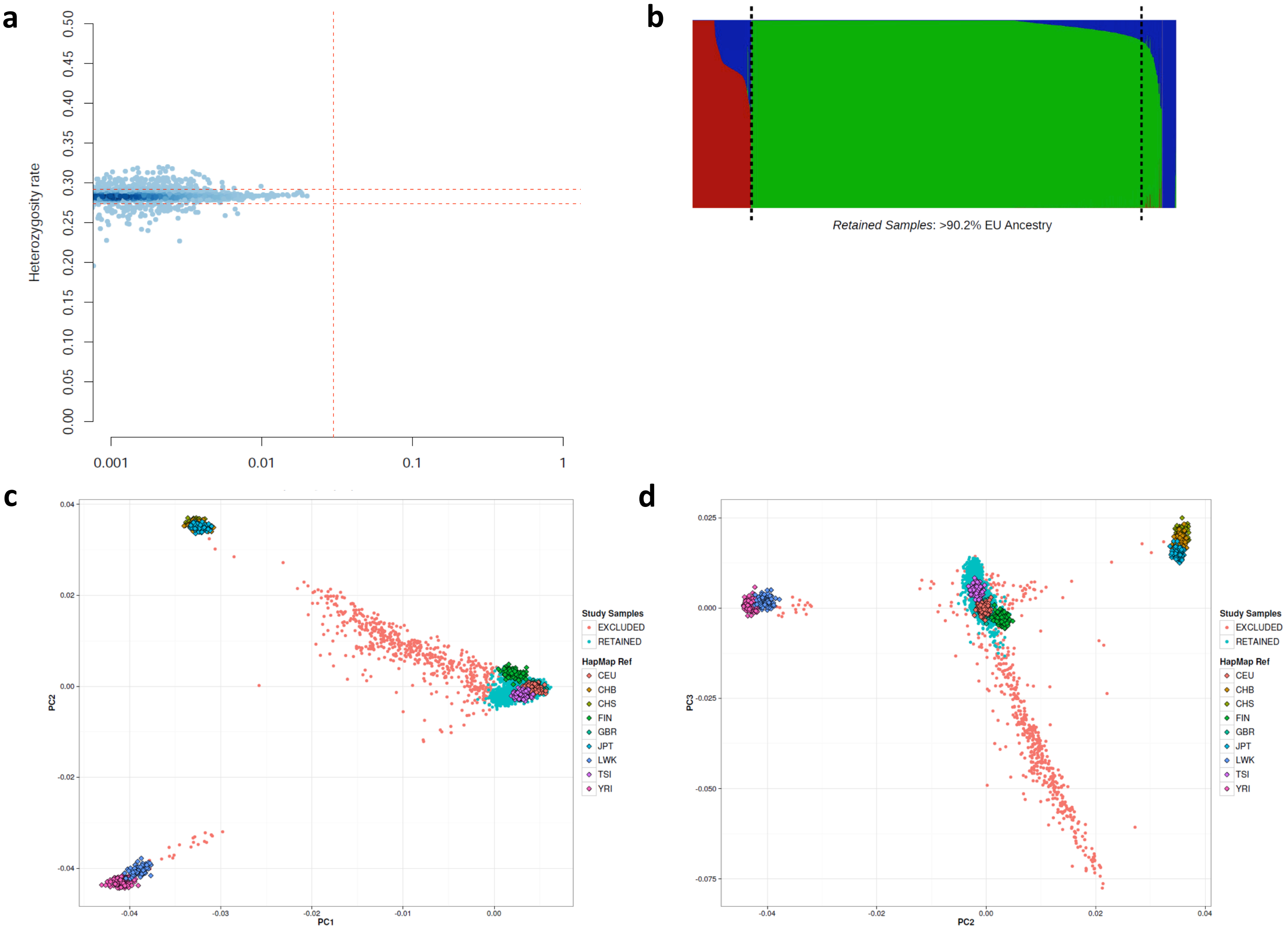

Supplementary Figure 2. SNP-based quality control and ancestry determination. (a) Exclusion of sample outliers based on heterozygosity, mean +/- 1.5 SD (red dotted lines). (b) Exclusion of non-European samples based on ethnicity estimation using fastStructure with HapMap continental groups and K=3 clustering. Samples with > 9.85% non-EU ancestry were excluded. This threshold was calibrated against the maximum of reference European groups CEU, GBR, and TSI. The results of principal component (PC) analysis for the cohort and reference groups are plotted along (c) PCs 1 and 2 and (d) PCs 2 and 3. Retained samples and excluded samples are shown in cyan and pink, respectively.

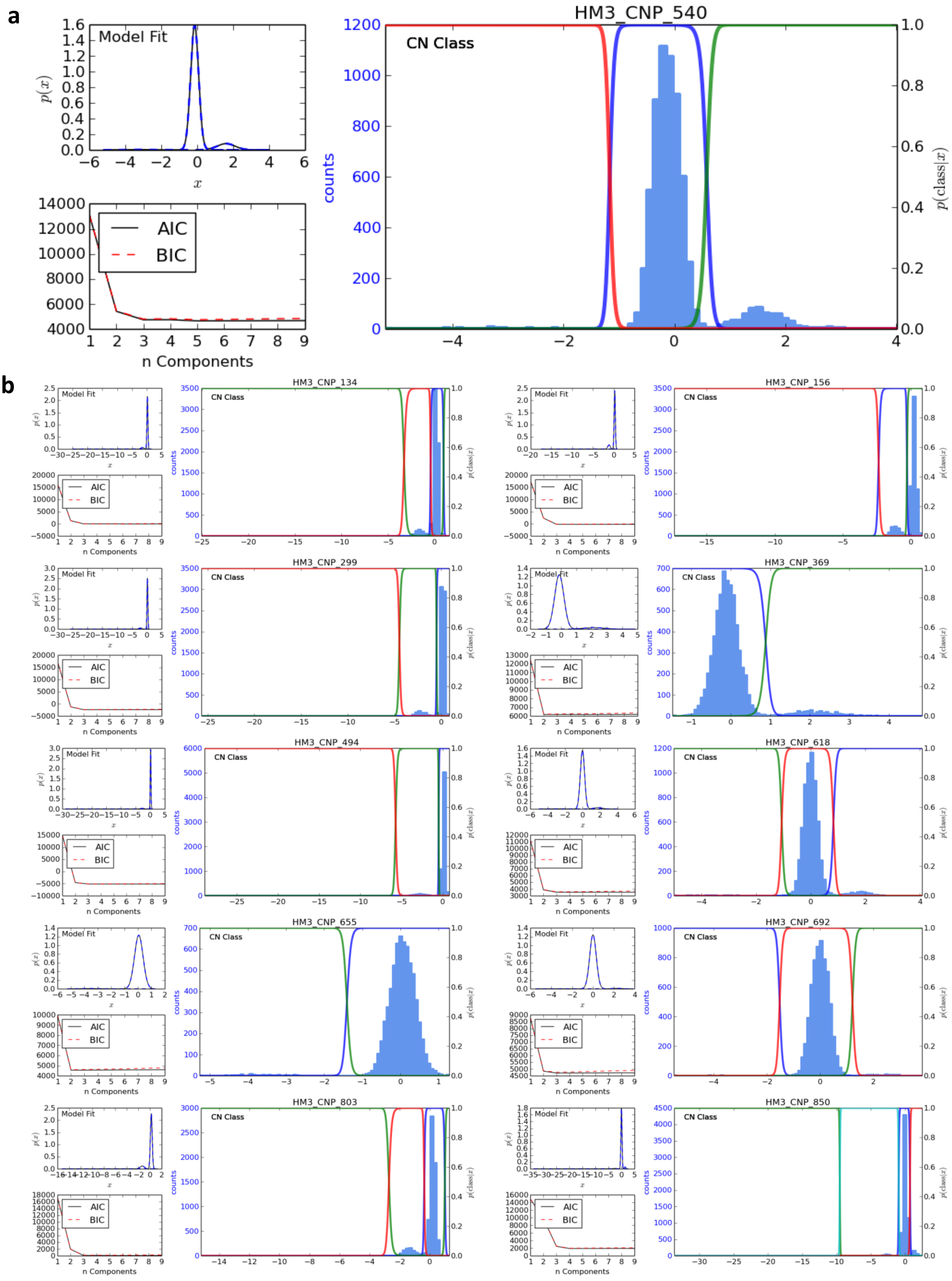
a
Model Fit
$p(x)$
x
AIC
BIC
n Components
HM3_CNP_540
CN Class
counts
$p(\text{class}|x)$
b
HM3_CNP_134
HM3_CNP_156
HM3_CNP_299
HM3_CNP_369
HM3_CNP_494
HM3_CNP_618
HM3_CNP_655
HM3_CNP_692
HM3_CNP_803
HM3_CNP_850

Supplementary Figure 3. Gaussian mixture model clusters of common HM3 CNVs. (a) A representative GMM cluster plot for locus HM3_CNP_540. Subplots for each CNV depict, counter-clockwise: the best-fit model, Akaike and Bayesian Information Criterion metrics calculated for GMM fitting 1-9 components, and the posterior probability for CNV cluster assignment (colored lines) overlaying the distribution of median summarized intensity values for all samples across region calculated using the best-fit model. (b) GMM plots for the 10 additional HapMap3 CNV loci that were used to critically evaluate sensitivity between cases and controls are displayed on the following page (Supplementary Methods and Supplementary Table 3).

Supplementary Table 3: GMM-based genotype calls at common CNV loci

CNV_ID	CLUSTER	CLUSTER_LRR	GMM_COPY	CTRL_CALLS	CASE_CALLS	CTRL_FREQ	CASE_FREQ	p-value
HM3_CNP_134	1	-13.17478812	0	7	4	0.002	0.002	1.0
HM3_CNP_134	2	-1.544234008	1	296	191	0.072	0.078	0.4
HM3_CNP_156	1	-1.141264855	1	517	315	0.126	0.129	0.7
HM3_CNP_156	2	-10.96495207	0	18	13	0.004	0.005	0.6
HM3_CNP_299	1	-2.148959932	1	275	142	0.067	0.058	0.2
HM3_CNP_299	2	-20.27406193	0	4	3	0.001	0.001	0.7
HM3_CNP_369	1	2.201328191	3	234	137	0.057	0.056	0.9
HM3_CNP_494	1	-2.7402128	1	196	100	0.048	0.041	0.2
HM3_CNP_494	2	-23.74078464	0	1	1	0.000	0.000	1.0
HM3_CNP_540	1	1.648736036	3	392	263	0.096	0.108	0.1
HM3_CNP_540	2	-3.301784945	1	32	17	0.008	0.007	0.8
HM3_CNP_618	1	-3.470922513	1	44	24	0.011	0.010	0.8
HM3_CNP_618	2	1.817743156	3	167	91	0.041	0.037	0.5
HM3_CNP_655	1	-3.645609914	1	45	34	0.011	0.014	0.3
HM3_CNP_692	0	-4.175170396	1	10	11	0.002	0.005	0.2
HM3_CNP_692	2	2.34262532	3	47	32	0.011	0.013	0.6
HM3_CNP_803	1	-10.64502833	0	15	14	0.004	0.006	0.2
HM3_CNP_803	2	-1.347106673	1	417	258	0.102	0.106	0.6
HM3_CNP_850	1	-31.82000658	0	1	1	0.000	0.000	1.0
HM3_CNP_850	2	-2.649145422	1	74	49	0.018	0.020	0.6
HM3_CNP_850	3	1.410233747	3	165	101	0.040	0.041	0.8

Supplementary Table 3. Gaussian Mixture Model (GMM) clustered genotype calls at common Hapmap 3 CNVs. For sensitivity analysis, all 6,535 samples used in this study were genotyped across 11 common Hapmap3 CNVs using a locus-specific GMM-based clustering method (see Supplementary Methods). The numbers for CNV_ID: Hapmap3 accession number. CLUSTER_ID: Arbitrary identifier assigned by the clustering algorithm. CLUSTER_LRR: The mean value of all median-summarized intensity values for all samples assigned to the cluster. CLUSTER_COPY: Copy-number state inferred by examination of raw LRR-intensity values for samples within the cluster. Call frequencies (FREQ) for 4,100 controls (CTRL) and 2,435 TS cases (CASE) reflect the proportion of GMM-based genotype calls with > 0.95 posterior probability of cluster assignment. There was no significant difference in CNV genotype frequency between phenotypic groups at any of the 21 non-reference genotype calls across all 11 loci (Fisher's exact test).

Supplementary Table 4a: Sensitivity analysis by locus

CNV_ID	CNV_TYPE	GMM_TOTAL	GMM_CTRL	GMM_CASE	HMM_CTRL	HMM_CASE	CTRL_SENSE	CASE_SENSE	p-value
HM3_CNP_134	DEL	498	303	195	300	194	0.990	0.995	1.0
HM3_CNP_156	DEL	863	535	328	531	321	0.993	0.979	0.11
HM3_CNP_299	DEL	424	279	145	279	145	1.000	1.000	1.0
HM3_CNP_369	DUP	371	234	137	208	122	0.889	0.891	1.0
HM3_CNP_494	DEL	298	197	101	197	101	1.000	1.000	1.0
HM3_CNP_540	DUP	655	392	263	391	261	0.997	0.992	0.57
HM3_CNP_540	DEL	49	32	17	32	17	1.000	1.000	1.0
HM3_CNP_618	DEL	68	44	24	44	24	1.000	1.000	1.0
HM3_CNP_618	DUP	258	167	91	166	90	0.994	0.989	1.0
HM3_CNP_655	DEL	79	45	34	45	34	1.000	1.000	1.0
HM3_CNP_692	DEL	21	10	11	10	11	1.000	1.000	1.0
HM3_CNP_692	DUP	79	47	32	47	32	1.000	1.000	1.0
HM3_CNP_803	DEL	704	432	272	428	272	0.991	1.000	0.16
HM3_CNP_850	DEL	125	75	50	75	50	1.000	1.000	1.0
HM3_CNP_850	DUP	266	165	101	164	98	0.994	0.970	0.15

Supplementary Table 4b: Overall sensitivity across common CNVs

CNV_TYPE	GMM_TOTALS	GMM_CTRL	GMM_CASE	HMM_CTRL	HMM_CASE	CTRL_SENSE	CASE_SENSE	p-value
DEL+DUP	4758	2957	1801	2917	1772	0.986	0.984	0.53
DEL	3129	1952	1177	1941	1169	0.994	0.993	0.81
DUP	1629	1005	624	976	603	0.971	0.966	0.65

Supplementary Table 4c: Group-wise sensitivity analysis across individuals

CNV_TYPE	CTRL_SENSE	Std. Error	CASE_SENSE	Std. Error	p-value
DEL+DUP	0.989	0.002	0.983	0.003	0.15
DEL	0.996	0.001	0.991	0.002	0.14
DUP	0.973	0.005	0.967	0.007	0.46

Supplementary Table 4. Sensitivity analysis of consensus HMM-segmentation calls. (a) Sensitivity by locus. The sensitivity HMM calling was defined as the number of concordant HMM calls divided by the total number of non-reference genotypes called in the same individual by GMM clustering. Non-reference GMM calls were collapsed into calls of the same class (CNV_TYPE, DEL or DUP). (b) Overall sensitivity across all loci. P-values for both individual and aggregated locus-specific locus-based tests were calculated using Fisher's exact test. (c) Group-wise comparison of sensitivity between cases and controls based on the average sensitivity calculated within each individual. No significant difference in the average individual sensitivity was observed between phenotypic groups whether considering deletions, duplications, or both in concert (Welch's *t*-test).

a

SAMPLE_ID	CHR	BP1	BP2	COPY	#SNPS	START_SNP	END_SNP	LRR-Z	$\mathrm{BAF}_{\mathrm{del}}$	$\mathrm{BAF}_{\mathrm{dup}}$	OUTLIER-Z
CNP_0348	6	67801176	67887156	1	21	rs9363696	rs16899159	-2.96	0.62	0.38	0.00015
CNP_0348[1]	**6**	**67907952**	**68586809**	**1**	**120**	**rs12197620**	**rs9354637**	**-2.9**	**0.76**	**0.16**	**0.00015**
CNP_0348	6	68707131	69142008	1	96	rs4707250	rs9363918	-2.93	0.73	0.17	0.00015
WT_0533[2]	**10**	**47375657**	**47703869**	**3**	**48**	**rs28599894**	**rs4434935**	**2.48**	**0.33**	**0.63**	**0.09**
CC_0852	10	47375657	47703869	3	48	rs28599894	rs4434935	2.36	0.33	0.60	0.09
WT_0866	10	47375657	47703869	3	48	rs28599894	rs4434935	2.33	0.38	0.60	0.09
TS_0457	10	47375657	47703869	3	48	rs28599894	rs4434935	2.29	0.39	0.60	0.09
TS_1843	10	47375657	47703869	3	48	rs28599894	rs4434935	2.05	0.39	0.60	0.09

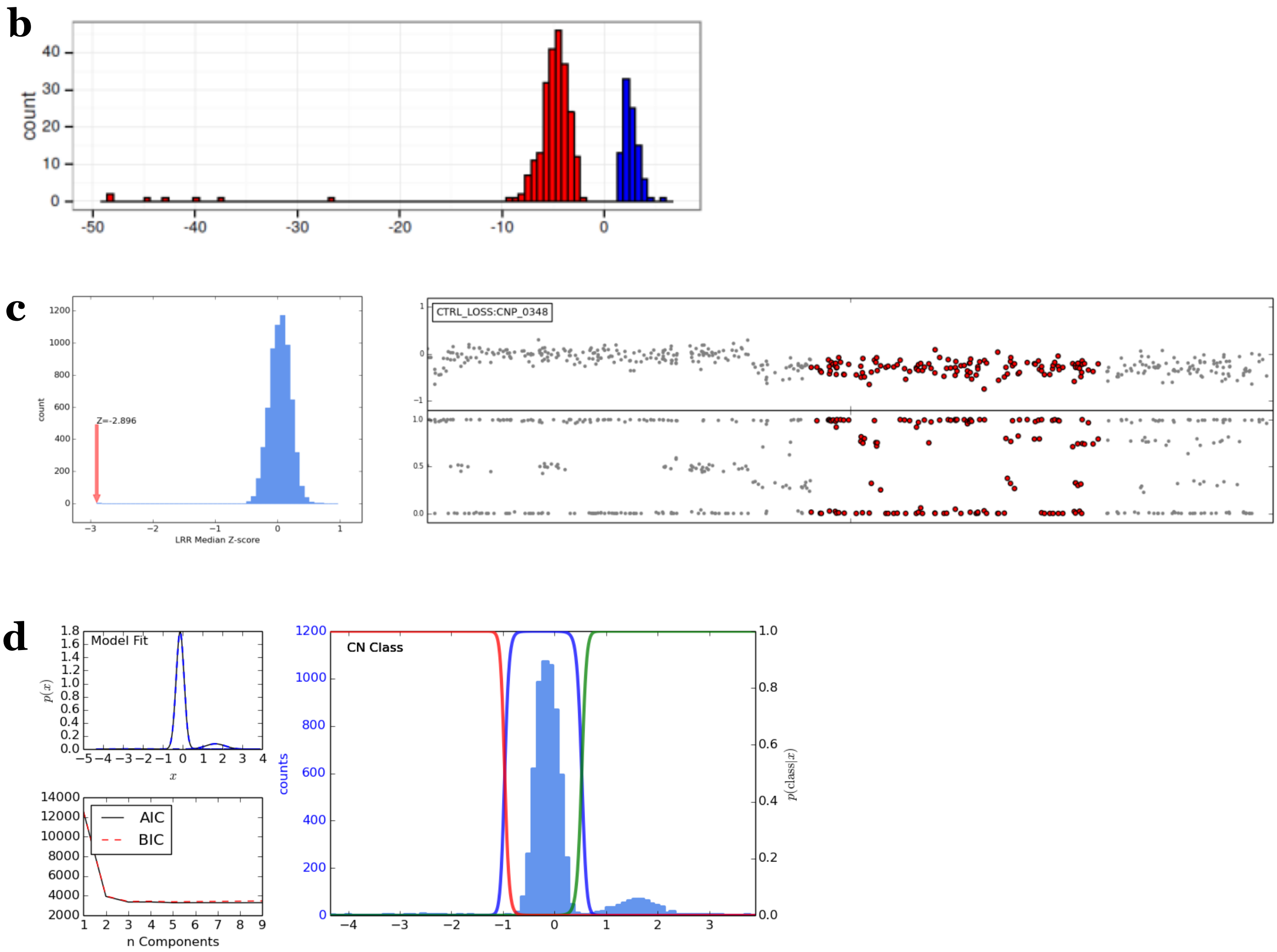

Supplementary Figure 4. In-silico validation of CNV calls. (a) Representative CNVs scored with various CNV validation metrics. Abbreviations (see Supplementary Methods for details): median summarized intensity measures across a putative CNV locus, standardized by sample (LRR-Z), proportion of probes with a BAF banding pattern indicative of a duplication event (BAF-D), proportion of samples with LRR-Z scores indicative of a polymorphic event (OUTLIER-Z). (b) Distribution of median summarized standardized intensity values (LRR-Z) for validated CNVs derived from HapMap samples generated on identical arrays as used in this study (Illumina OmniExpress). Based on this distribution, CNVs without an LRR-Z score < 2.3 (deletions) and > 1.3 (duplications) were flagged for manual inspection. (c) Example of a large singleton mosaic event flagged for exclusion in sample CNP_0348, indicated as (1) in Figure 4a. This CNV on chromosome 6 was detected as three separate CNVs after taking the consensus of two different HMM calling algorithms. The largest CNV call exhibits an LRR-Z score of -2.86 (left, red arrow), indicative of a deletion, but shows a clear BAF-banding pattern of a duplication event (right), with a BAF_{dup} score of 0.16. This is indicative of a mosaic event, where only a proportion of cells from sample CNP_0348 harbor the deletion event. (d) Example of a polymorphic CNV on chr10:47,375,657-47,703,869 misclassified as a rare event due to reduced sensitivity, indicated as (2) in Figure 4a, with an OUTLIER-Z score of 0.09. Genotyping using GMM-based clustering indicated that this misclassified rare event (MAF < 0.01) has a MAF of 0.12.

Supplementary Table 5a: Burden per CNV

		RARE CNVS			SINGLETONS		
SIZE CATEGORY	**CNV TYPE**	**OR**	**95% CI**	**p-value**	**OR**	**95% CI**	**p-value**
ALL	DEL+DUP	1.01	[0.97-1.06]	0.60	1.09	[1.01-1.18]	0.03
	DEL	1.03	[0.96-1.10]	0.41	1.12	[0.99-1.26]	0.06
	DUP	1.00	[0.94-1.06]	0.97	1.07	[0.96-1.9]	0.18
>500KB	DEL+DUP	1.19	[1.01-1.41]	0.04	1.30	[1.01-1.67]	0.04
	DEL	1.21	[0.86-1.71]	0.26	1.72	[1.06-2.83]	0.03
	DUP	1.18	[0.98-1.43]	0.09	1.17	[0.86-1.57]	0.32
>1MB	DEL+DUP	1.50	[1.10-2.03]	0.009	1.91	[1.24-2.97]	0.004
	DEL	1.85	[1.06-3.25]	0.03	2.82	[1.36-6.18]	0.007
	DUP	1.37	[0.95-1.96]	0.09	1.53	[0.89-2.64]	0.12

Supplementary Table 5b: Burden per 100KB of CNV length

		RARE CNVS			SINGLETONS		
SIZE CATEGORY	**CNV TYPE**	**OR**	**95% CI**	**p-value**	**OR**	**95% CI**	**p-value**
ALL	DEL+DUP	1.011	[1-1.021]	0.05	1.022	[1.006-1.035]	0.006
	DEL	1.017	[0.997-1.037]	0.09	1.027	[1.003-1.055]	0.04
	DUP	1.008	[0.995-1.021]	0.22	1.016	[1-1.034]	0.06
>500KB	DEL+DUP	1.015	[1.003-1.027]	0.01	1.021	[1.006-1.037]	0.006
	DEL	1.016	[0.994-1.039]	0.16	1.029	[1-1.059]	0.06
	DUP	1.015	[1.001-1.029]	0.04	1.017	[1-1.039]	0.06
>1MB	DEL+DUP	1.018	[1.005-1.032]	0.007	1.024	[1.007-1.043]	0.008
	DEL	1.025	[1.001-1.052]	0.05	1.029	[1.005-1.064]	0.06
	DUP	1.015	[1-1.032]	0.05	1.021	[1.002-1.044]	0.05

Supplementary Table 5c: Burden per gene

		RARE CNVS			SINGLETONS		
SIZE CATEGORY	**CNV TYPE**	**OR**	**95% CI**	**p-value**	**OR**	**95% CI**	**p-value**
ALL	DEL+DUP	1.008	[1-1.016]	0.06	1.016	[1.004-1.030]	0.01
	DEL	1.012	[0.991-1.033]	0.27	1.023	[0.989-1.059]	0.18
	DUP	1.007	[0.999-1.016]	0.10	1.015	[1.002-1.030]	0.03
>500KB	DEL+DUP	1.012	[1.003-1.022]	0.01	1.019	[1.005-1.036]	0.03
	DEL	1.008	[0.982-1.034]	0.53	1.024	[0.984-1.066]	0.39
	DUP	1.012	[1.002-1.023]	0.02	1.018	[1.004-1.037]	0.04
>1MB	DEL+DUP	1.014	[1.004-1.026]	0.01	1.022	[1.008-1.044]	0.02
	DEL	1.021	[0.989-1.054]	0.20	1.036	[0.991-1.081]	0.27
	DUP	1.013	[1.002-1.025]	0.02	1.022	[1.005-1.044]	0.04

Supplementary Table 5. Analysis of global CNV burden. Comparison of genome-wide CNV burden among TS cases compared to controls, as defined by (a) total number of CNVs (b) 100-kbp of CNV length, and (c) the total number of genes affected by CNVs, stratified by CNV frequency, size and type. Odds ratios indicate an increased risk for TS per unit of CNV burden, and were calculated using logistic regression with covariates significantly associated with any of the CNV burden metrics used, both for total CNV burden as well as burden due to small CNV events (see Supplementary Methods). P-values were calculated using the likelihood ratio test. Singletons are defined as CNVs occurring only once among either a single case or control. Event counts are based on a 50% reciprocal overlap. Gene counts are defined as the number of Refseq genes overlapping CNVs by any amount.

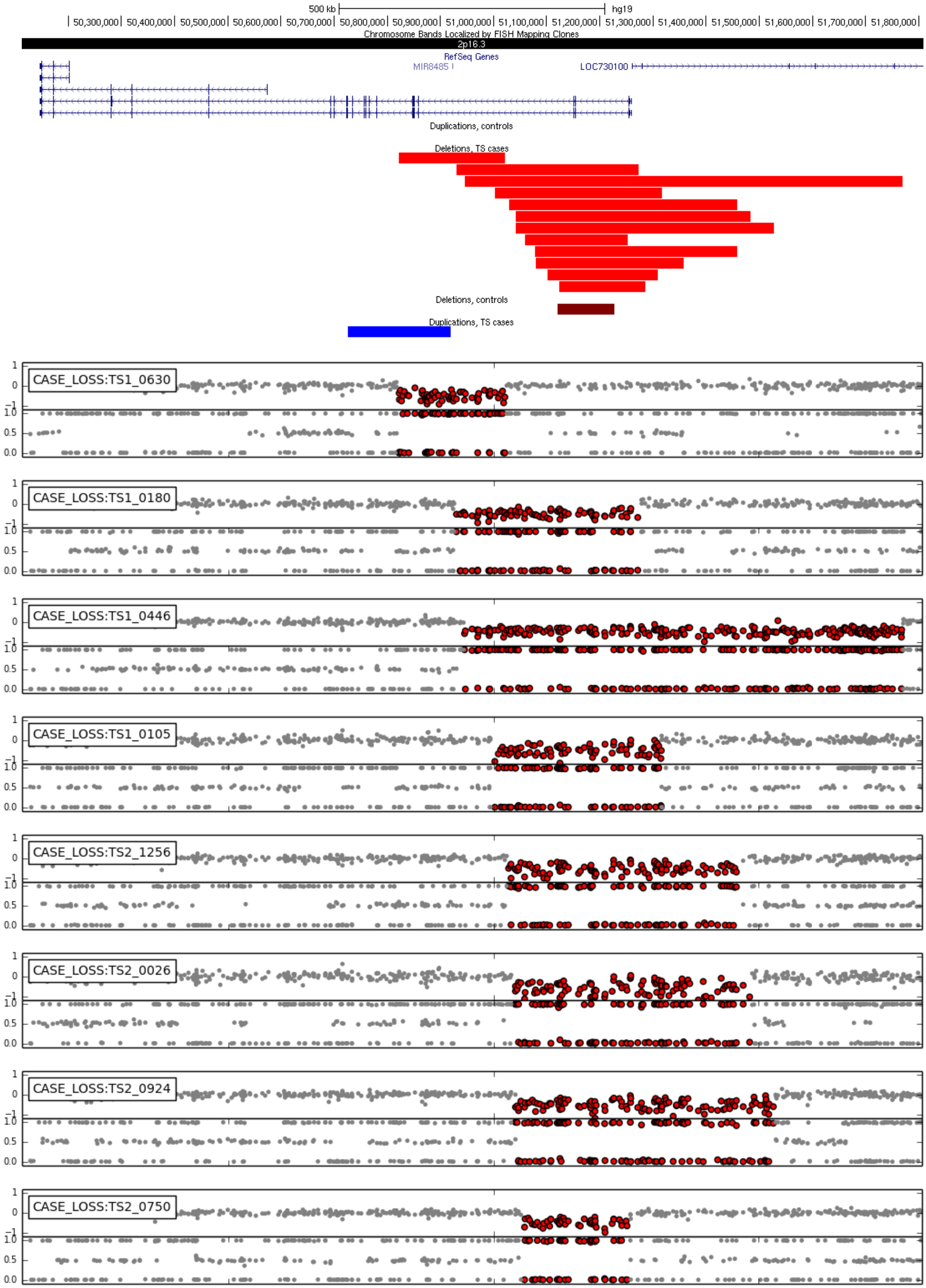
500 kb
hg19
50,300,000
50,400,000
50,500,000
50,600,000
50,700,000
50,800,000
50,900,000
51,000,000
51,100,000
51,200,000
51,300,000
51,400,000
51,500,000
51,600,000
51,700,000
51,800,000
Chromosome Bands Localized by FISH Mapping Clones
2p16.3
RefSeq Genes
MIR8485
LOC730100
Duplications, controls
Deletions, TS cases
Deletions, controls
Duplications, TS cases
CASE_LOSS:TS1_0630
CASE_LOSS:TS1_0180
CASE_LOSS:TS1_0446
CASE_LOSS:TS1_0105
CASE_LOSS:TS2_1256
CASE_LOSS:TS2_0026
CASE_LOSS:TS2_0924
CASE_LOSS:TS2_0750
1
0
-1
1.0
0.5
0.0

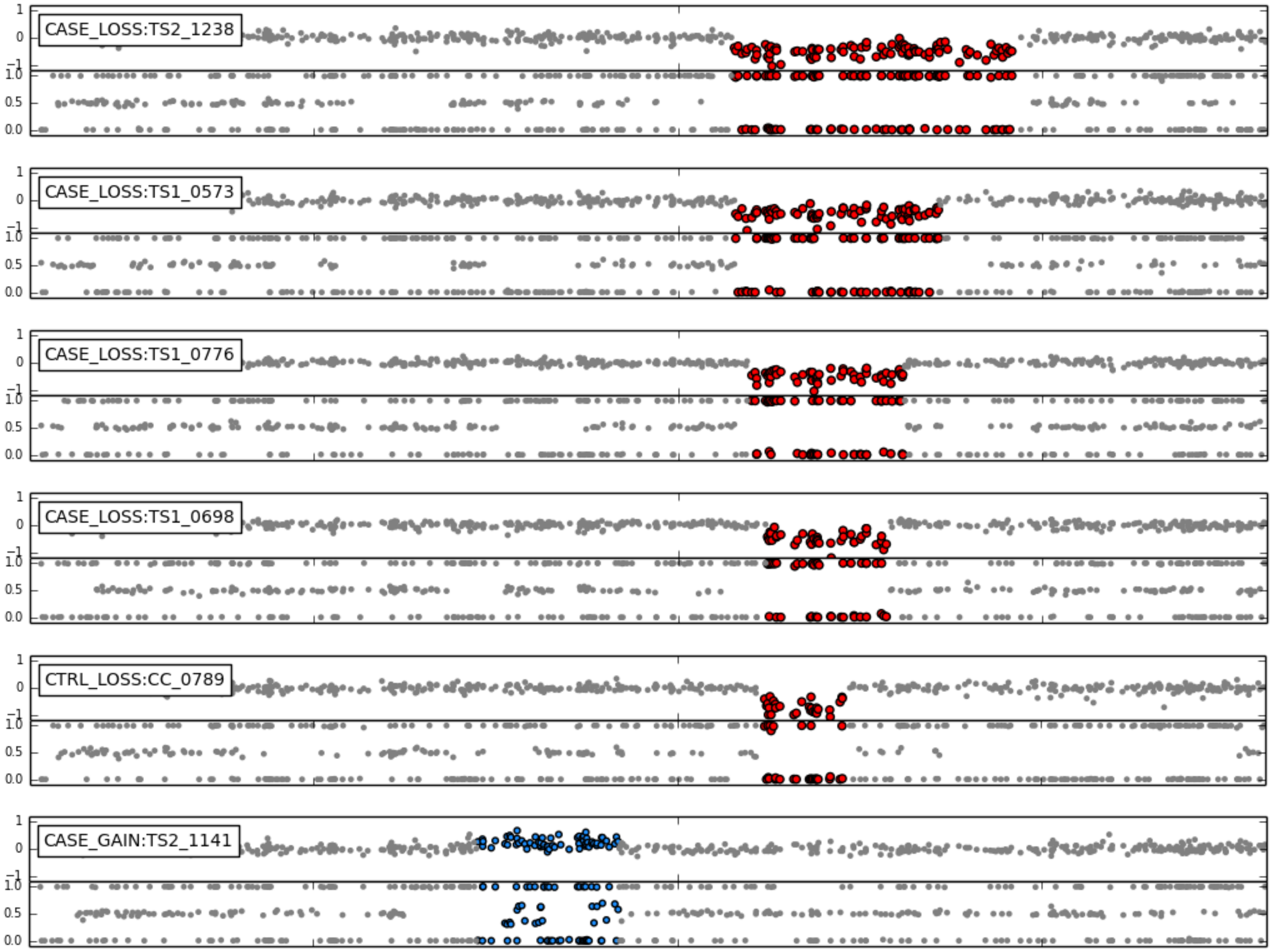

Supplementary Figure 6. Exonic CNVs affecting *NRXN1*. UCSC genome browser track depicting all exonic *NRXN1* CNVs > 50kb identified in this study: 12 heterozygous case deletions (red), one control deletion (dark red) and a single case duplication (blue). Probe-level plots of LRR intensity and BAF for all exonic *NRXN1* CNV carriers shown in the same order as the UCSC genome browser track. Colored probes indicate the location of called deletions (red) and duplications (blue).

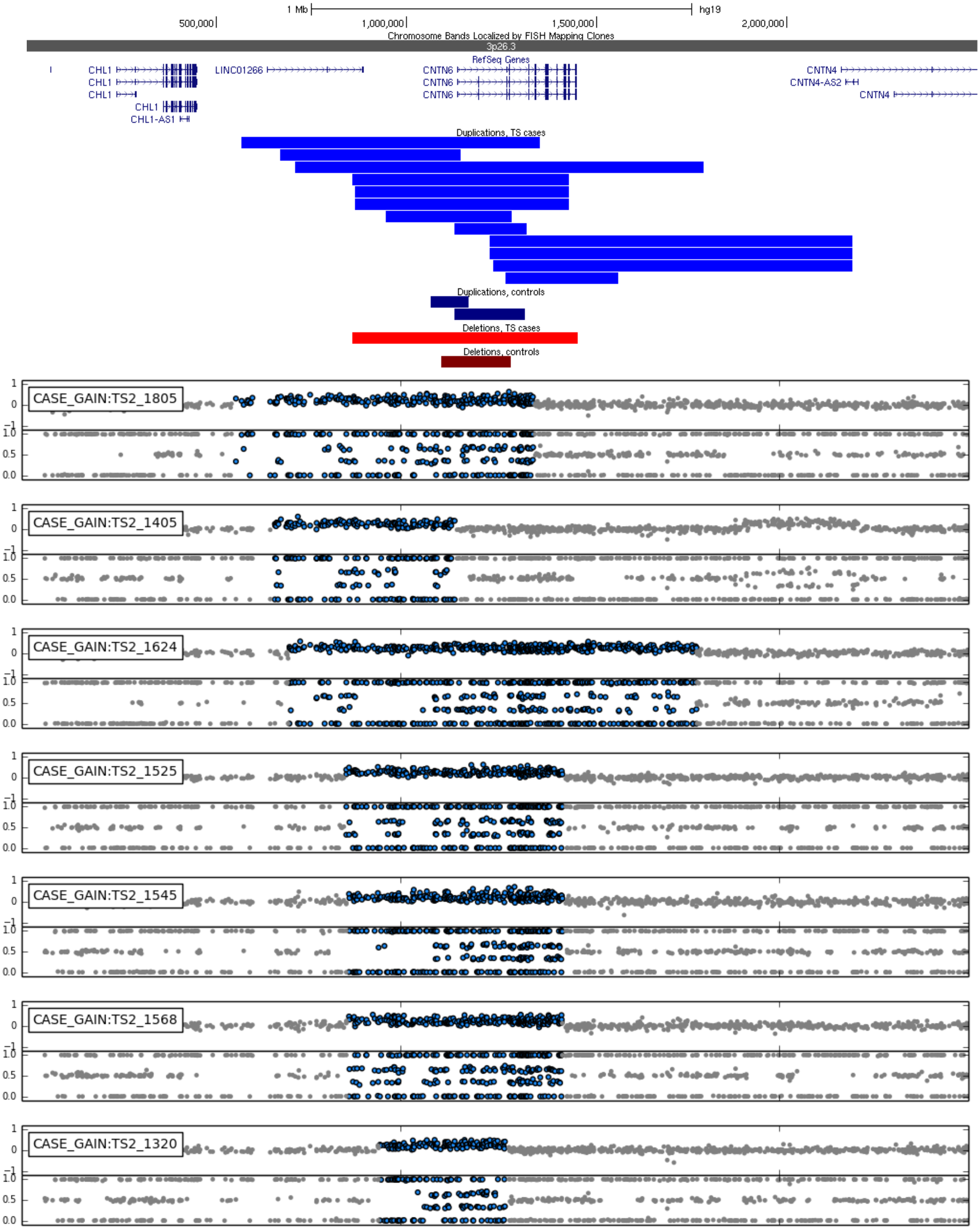
1 Mb
hg19
500,000
1,000,000
1,500,000
2,000,000
Chromosome Bands Localized by FISH Mapping Clones
3p26.3
RefSeq Genes
CHL1
CHL1
CHL1
CHL1
CHL1-AS1
LINC01266
CNTN6
CNTN6
CNTN6
CNTN4
CNTN4-AS2
CNTN4
Duplications, TS cases
Duplications, controls
Deletions, TS cases
Deletions, controls
CASE_GAIN:TS2_1805
CASE_GAIN:TS2_1405
CASE_GAIN:TS2_1624
CASE_GAIN:TS2_1525
CASE_GAIN:TS2_1545
CASE_GAIN:TS2_1568
CASE_GAIN:TS2_1320
1
0
-1
1.0
0.5
0.0

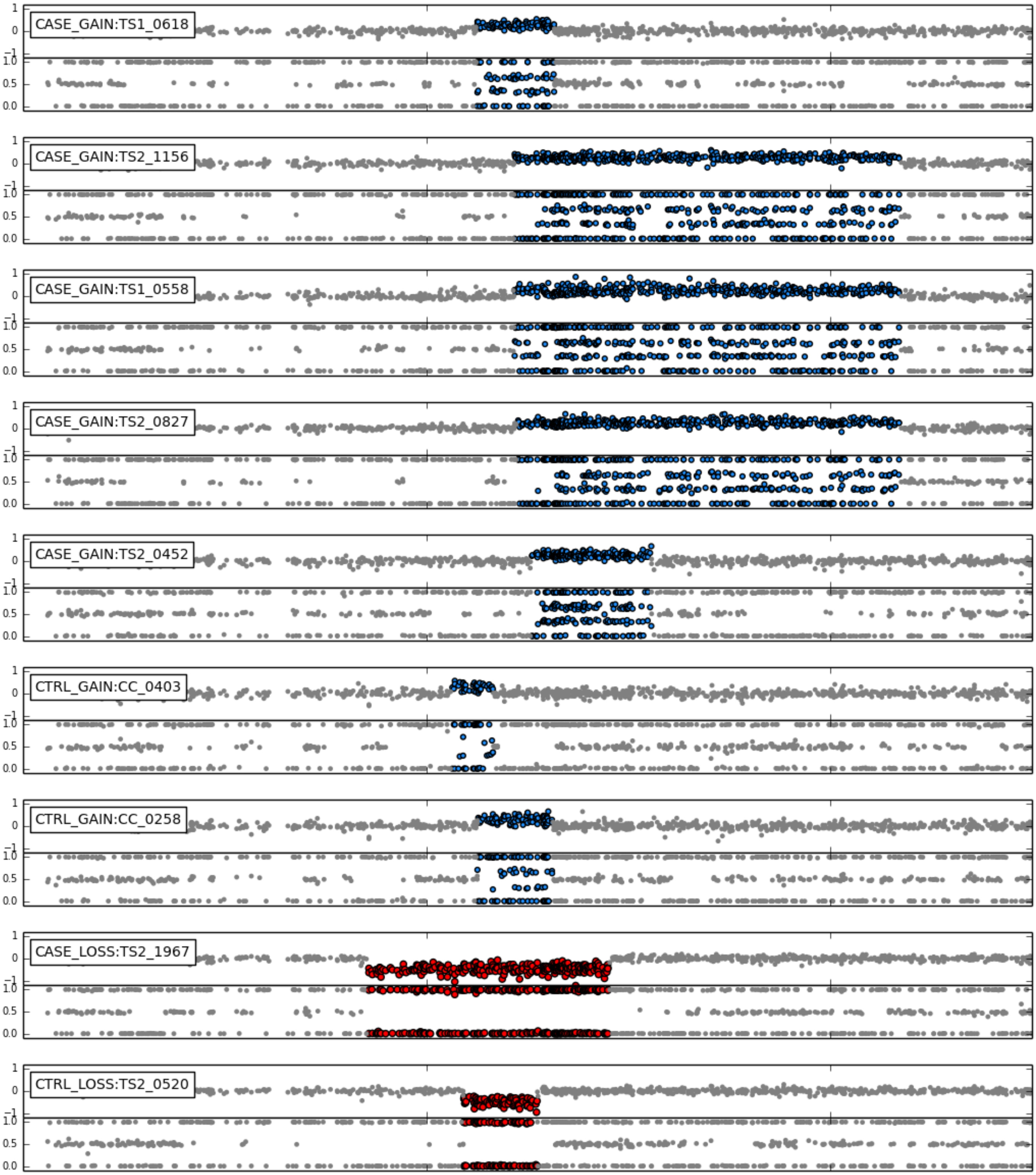
CASE_GAIN:TS1_0618
CASE_GAIN:TS2_1156
CASE_GAIN:TS1_0558
CASE_GAIN:TS2_0827
CASE_GAIN:TS2_0452
CTRL_GAIN:CC_0403
CTRL_GAIN:CC_0258
CASE_LOSS:TS2_1967
CTRL_LOSS:TS2_0520
1
0
−1
1.0
0.5
0.0

Supplementary Figure 7. CNVs overlapping *CNTN6*. UCSC genome browser track displaying heterozygous genic duplications in TS cases (blue) and controls (dark blue) followed by deletions (red). Probe-level LRR and BAF plots for all 16 CNVs detected spanning *CNTN6* are shown below.

Supplementary Table 6: Nominally significant results from gene-based association

LOCUS	TYPE	LOCATION	CTRL_FREQ	CASE_FREQ	P_{locus}	P_{corr}
NRXN1	DEL	chr2:50145642-51259674	12	1	6.2e-5	6.7e-4
CALY	DEL	chr10:135138927-135150475	4	0	0.019	0.50
PRAP1	DEL	chr10:135160843-135166187	4	0	0.019	0.50
ZNF511	DEL	chr19:53935226-53947925	4	0	0.019	0.50
CNTN6	DUP	chr3:1134341-1445292	12	2	2.5e-4	8.3e-3
CNTN4	DUP	chr3:2140549-3099645	8	3	0.018	0.93
SHCBP1	DUP	chr16:46614467-46655311	4	0	0.019	0.90
VPS35	DUP	chr16:46693588-46723144	4	0	0.019	0.90
ORC6	DUP	chr16:46723557-46732306	4	0	0.019	0.90
IGSF11	DUP	chr3:118619478-118864898	18	15	0.032	1.0
SPSB1	DUP	chr1:9352940-9429590	25	25	0.044	1.0
RPL38	DUP	chr17:72199721-72206794	12	9	0.050	1.0
TTYH2	DUP	chr17:72209653-72258155	12	9	0.050	1.0
DNAI2	DUP	chr17:72270386-72311023	12	9	0.050	1.0
KIF19	DUP	chr17:72322349-72351959	12	9	0.050	1.0
BTBD17	DUP	chr17:72352555-72358085	12	9	0.050	1.0
GPR142	DUP	chr17:72363546-72368761	12	9	0.050	1.0
GPRC5C	DUP	chr17:72420990-72447792	12	9	0.050	1.0
CD300A	DUP	chr17:72462555-72480933	12	9	0.050	1.0
CD300LB	DUP	chr17:72517313-72527613	12	9	0.050	1.0
CD300C	DUP	chr17:72537247-72542282	12	9	0.050	1.0
CD300LD	DUP	chr17:72575504-72588422	12	9	0.050	1.0
C17orf77	DUP	chr17:72580818-72590348	12	9	0.050	1.0
CD300E	DUP	chr17:72606026-72619897	12	9	0.050	1.0

Supplementary Table 6. All nominally significant results from gene-based association test. Gene-based association was conditioned on CNVs spanning exons of protein-coding genes, as determined by strict overlap with Refseq annotation. Significance was established using 1,000,000 permutations (P_{locus}), using the max(T) method to establish genome-wide significance, corrected for multiple testing (P_{corr}). Duplications and deletions were independently filtered for a MAF <0.01, and tested independently.

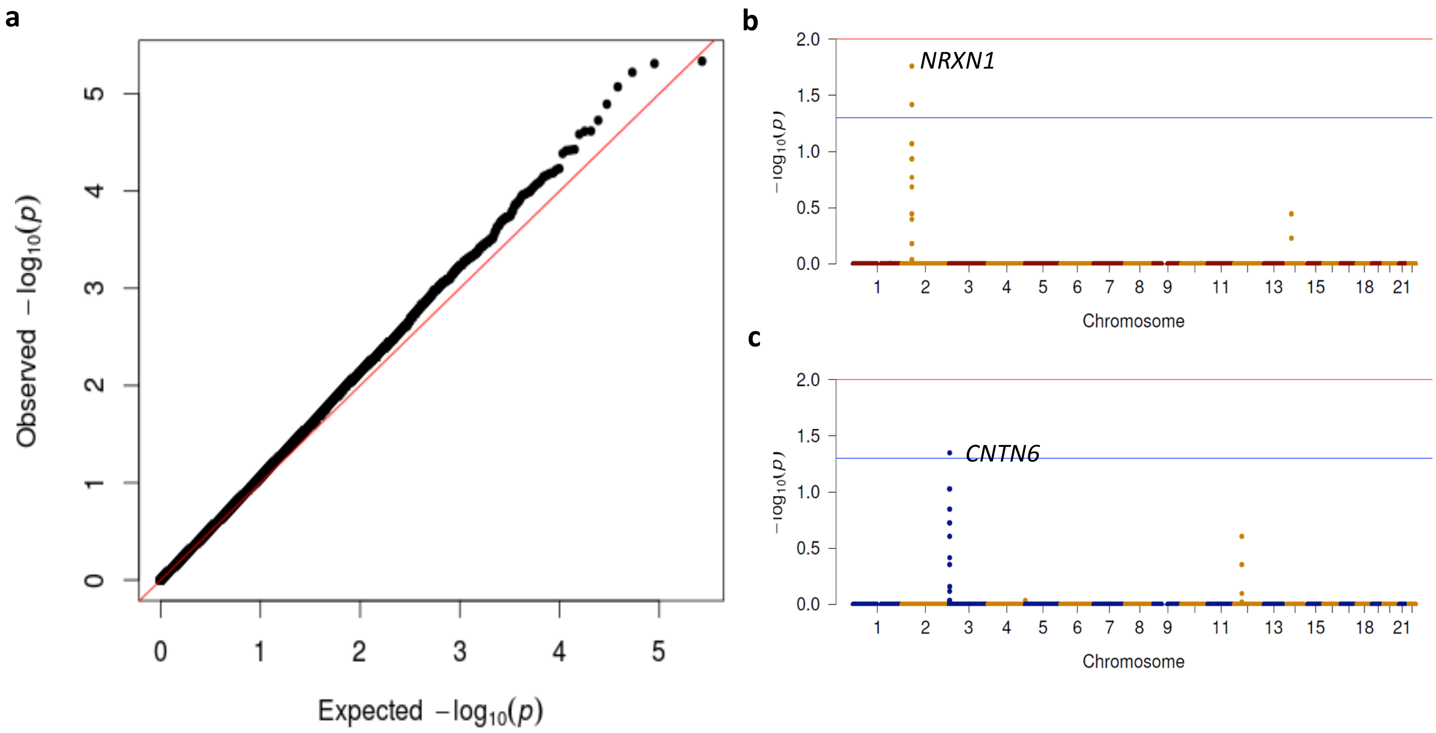

Supplementary Figure 8. Examination for population-specific effects. To verify the robustness of our results to population stratification, we pair-matched each case subject with exactly one case such that the global difference between all pairs is minimized using SpectralGEM. We also excluded all outlying pairs based on the genetic distance between them (>90th percentile). (a) The SNP-based λ_{gc} of the resultant dataset (1996 cases and 1996 controls) was an acceptable 1.082. Manhattan plots of segmental association results demonstrate that (b) deletions in *NRXN1* and (c) duplications in *CNTN6* are significant with an α < 0.05 (blue line). Deletions and duplications were analyzed separately. The -log10 (p-value) displayed is empirically corrected for FWER genome-wide using the max(T) method with 1,000,000 permutations.

Supplementary Table 7: Prevalence of known, recurrent, pathogenic CNVs in TS

LOCUS	LOCATION (hg19)	CNV	CASE	CTRL	EMP-P	EMP-P
		TYPE	FREQ	FREQ	(1-sided)	(2-sided)
1q21.1	1:146089254-147859944	Loss	1	1	0.62(1)	
3q29	3:195766737-197216349	Loss	0	0	1(1)	
7q36.3 (VIPR2)	7:157860945-159119486	Loss	0	0	1(1)	
10q11.22-23	10:46508694-51912781	Loss	0	0	1(1)	
15q11.2	15:22750305-23272733	Loss	10	8	0.1(0.59)	
15q13.1	15:28973396-30556183	Loss	0	0	1(1)	
15q13.3	15:30936285-32620127	Loss	0	1	1(1)	
16p13.11	16:15125441-16291983	Loss	1	1	0.62(1)	
16p12.1	16:21947230-22423698	Loss	1	1	0.62(1)	
16p11.2 distal	16:28814098-29043450	Loss	0	0	1(1)	
16p11.2	16:29595483-30192561	Loss	2	2	0.5(0.98)	
17p12	17:14101029-15471179	Loss	1	0	0.39(0.94)	
17q12	17:34815551-36249430	Loss	0	1	1(1)	1(1)
22q11.21 short	22:18905281-21488855	Loss	0	0	1(1)	
22q11.21 long	22:20733495-21465780	Loss	1	0	0.39(0.94)	
1q21.1	1:146089254-147859944	Gain	2	3	0.63(1)	1(1)
2p25.3	2:1754610-2225144	Gain	0	0	1(1)	
7q36.3 (VIPR2)	7:158726462-158947294	Gain	0	1	1(1)	1(1)
10q11.22-23	10:47543322-51912781	Gain	0	0	1(1)	
13q31.3	13:94358193-94419894	Gain	0	0	1(1)	
15q11.2-13.1	15:22770994-28535266	Gain	2	0	0.15(0.35)	
15q13.1	15:29562640-30689724	Gain	0	0	1(1)	
16p13.11	16:14989844-16291983	Gain	1	6	1(1)	0.26(0.73)
16p11.2	16:29624247-30198151	Gain	0	1	1(1)	1(1)
17q12	17:34815551-36249430	Gain	2	2	0.5(0.94)	
22q11.21 short	22:18905281-21488855	Gain	3	4	0.54(0.99)	
22q11.21 long	22:20718116-21465780	Gain	0	0	1(1)	

Supplementary Table 7. Prevalence of known, recurrent, neuropsychiatric CNVs in TS. Known CNVs were considered present in a sample if it carried a variant of the same CNV type (deletion/duplication) and overlapped at least 50% the length of the known recurrent CNV, except for the single-gene locus containing *VIPR2*, where the associated signal has been shown to derive from non-recurrent events[37]. For this locus, any CNV > 50kb overlapping any portion of the gene was counted. P-values were determined with 100,000 permutations using the max(T) method to control for the family-wise error rate. P-values corrected empirically for multiple testing are shown in parentheses, with two-sided p-values presented only when there is enrichment in controls.

Supplementary Table 8: Clinical phenotypes of *NRXN1* and *CNTN6* CNV carriers

SAMPLE_ID	GENE	CHR	START	END	CNV_TYPE	LENGTH_KB	CNV_EFFECT	OCD	ADHD	FLAGGED	NOTES
TS1_0630	NRXN1	2	50821559	51021488	DEL	199.9	CODING	1	1	Y	Unspecified Developmental Delay (ICD-9: 315.9)
TS1_0180	NRXN1	2	50930181	51272375	DEL	342.2	CODING	1	1	Y	Asperger Syndrome
TS1_0446	NRXN1	2	50945471	51770480	DEL	825	CODING	2	2	N	
TS1_0105	NRXN1	2	51002606	51316822	DEL	314.2	CODING	1	2	N	
TS2_1256	NRXN1	2	51028662	51458570	DEL	429.9	CODING	1	2	Y	Other developmental speech or language disorder (ICD-9: 315.39)
TS2_0026	NRXN1	2	51041472	51483528	DEL	442.1	CODING	1	1	N	
TS2_0924	NRXN1	2	51041603	51528298	DEL	486.7	CODING	1	2	N	
TS2_0750	NRXN1	2	51058745	51252137	DEL	193.4	CODING	2	2	Y	Asperger Syndrome
TS2_1238	NRXN1	2	51077569	51458570	DEL	381	CODING	2	1	Y	Paranoid personality disorder
TS1_0573	NRXN1	2	51079482	51357902	DEL	278.4	CODING	NA	NA	NA	
TS1_0776	NRXN1	2	51101583	51308895	DEL	207.3	CODING	1	2	N	Brother with Asperger Syndrome
TS1_0698	NRXN1	2	51123048	51286169	DEL	163.1	CODING	2	2	N	
TS2_1805	CNTN6	3	565961	1350458	DUP	784.5	CODING	2	NA	N	
TS2_1405	CNTN6	3	668832	1143424	DUP	474.6	5' UTR	2	2	N	
TS2_1624	CNTN6	3	707257	1781739	DUP	1074	CODING	1	1	N	
TS2_1525	CNTN6	3	857325	1427769	DUP	570.4	CODING	2	2	N	
TS2_1568	CNTN6	3	864513	1425997	DUP	561.5	CODING	2	2	N	
TS2_1545	CNTN6	3	864513	1427769	DUP	563.3	CODING	1	2	N	
TS2_1320	CNTN6	3	946290	1276092	DUP	329.8	CODING	2	1	N	
TS1_0618	CNTN6	3	1125605	1315900	DUP	190.3	CODING	1	1	N	
TS2_1156	CNTN6	3	1218279	2170519	DUP	952.2	CODING	1	2	N	
TS1_0558	CNTN6	3	1218279	2170519	DUP	952.2	CODING	1	2	N	
TS2_0827	CNTN6	3	1226953	2170519	DUP	943.6	CODING	1	1	N	
TS2_0452	CNTN6	3	1260932	1556680	DUP	295.7	CODING	1	1	N	

Supplementary Table 8. Clinical phenotypes of *NRXN1* and *CNTN6* CNV carriers. Clinical phenotypes for all CNV carriers of the two significant TS loci detected in this study (gene-based association test): Deletions at *NRXN1* and duplications at *CNTN6*, including common comorbid disorders for TS, attention deficit disorder (ADHD) and obsessive compulsive disorder (OCD) as well as whether or not the individual was flagged for an atypical phenotype (FLAGGED, and described in NOTES).

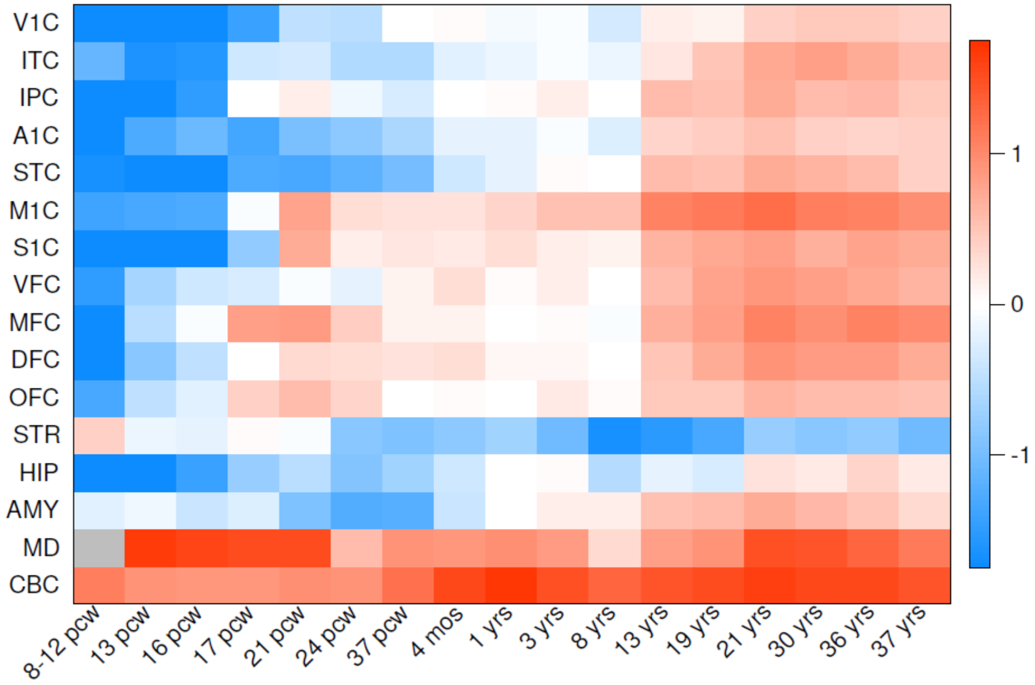

Supplementary Figure 9. Spatio-temporal expression of *CNTN6* in human brain. Analysis of RNASeq data from Brainspan (www.brainspan.org) indicates that *CNTN6* is most highly expressed postnatally in the cerebellum (CBC) followed by the thalamus (MD). Heatmap represents median expression values for all available samples at each tissue normalized across each developmental timepoint. Regions: primary visual cortex (V1C), inferolateral temporal cortex (ITC), posteroventral parietal cortex (IPC), primary auditory cortex (A1C), posterior superior temporal cortex (STC), primary motor cortex (M1C), primary somatosensory cortex (S1C), ventrolateral prefrontal cortex (VFC), anterior cingulate cortex (MFC), dorsolateral prefrontal cortex (DFC), orbital frontal cortex (OFC), striatum (STR), hippocampus (HIP), amygdaloid complex (AMY), mediodorsal nucleus of thalamus (MD), cerebellar cortex (CBC). Temporal abbreviations: post-conception weeks (pcw), months (mos), years (yrs).

a

Global CNV burden: CNV number

	Estimate	Std. Error	t value	Pr(>|t|)	
(Intercept)	2.667865	0.401367	6.647	3.23E-11	***
BATCH	0.003681	0.04171	0.088	0.9297	
SNPSEX	0.048885	0.16275	0.3	0.7639	
LRRSD	-0.478306	3.96538	-0.121	0.904	
PC1	-3.830912	15.6941	-0.244	0.8072	
PC2	-0.946009	12.313217	-0.077	0.9388	
PC3	-13.723276	7.559477	-1.815	0.0695	
PC4	16.790214	27.263604	0.616	0.538	
PC5	-1.487214	26.446038	-0.056	0.9552	
PC6	3.651484	26.630104	0.137	0.8909	
PC7	13.741436	25.170284	0.546	0.5851	
PC8	-2.461499	11.018938	-0.223	0.8232	
PC9	12.812941	10.154253	1.262	0.2071	
PC10	-6.114161	17.290363	-0.354	0.7236	

b

Small CNV burden: CNV number

	Estimate	Std. Error	t value	Pr(>|t|)	
(Intercept)	6.90E-01	5.60E-02	12.323	<2e-16	***
BATCH	1.93E-05	5.84E-03	0.003	0.9974	
SNPSEX	-4.92E-03	2.28E-02	-0.216	0.8289	
LRRSD	**1.21E+00**	**5.52E-01**	**2.192**	**0.0284**	*
PC1	2.41E+00	2.20E+00	1.096	0.2731	
PC2	3.09E+00	1.72E+00	1.795	0.0728	
PC3	1.23E-01	1.06E+00	0.116	0.9076	

c

Small CNV burden: Total CNV length

	Estimate	Std. Error	t value	Pr(>|t|)	
(Intercept)	0.76814	0.10909	7.041	2.10E-16	***
BATCH	-0.01947	0.01138	-1.712	0.087	
SNPSEX	0.02371	0.04436	0.535	0.593	
LRRSD	**2.25759**	**1.07506**	**2.1**	**0.0358**	*
PC1	-0.83495	4.28069	-0.195	0.8454	
PC2	0.64946	3.35755	0.193	0.8466	
PC3	-1.82731	2.05692	-0.888	0.3744	

Supplementary Table 9. Regression models of global CNV burden. (a) Results from a linear regression model of global burden with total CNV count as the dependent variable, and genotyping batch, subject sex, LogR-Ratio standard deviation (LRRSD, a general metric for CNV assay quality), and the top 10 ancestry PCs as dependent variables. None of the included covariates were significant predictors of global CNV burden in terms of CNV count or total CNV size (Supplementary Text). However, when restricted to small CNV events (<100kb), LRRSD was a significant predictor of CNV burden in terms of (b) total CNV count and (c) total CNV length; therefore LRRSD was included as a covariate in our subsequent analysis.